



# **Simplistic Transient and non-uniform stress analysis of silicone breast Implant to Tackle Vascular Contracture**

Group 3, Supervisor Dr. Kateryna Bazaka

**Ar kar Nyan Hein-n8709041**

**Ziyan Guo-n10054553**

**Hamza Malik-n10240420**

**Keyur Kanubhai Patel-n10176896**

**Yi-Chen Hsu- n9806733**

**Bhavin Jieshbhai Vyas- n10017518**

**Naveen Paruchuri- n10327894**

## Contents

<b>Executive Summary</b>	<b>9</b>
<b>1.0 Introduction</b>	<b>11</b>
<b>2.0 Literature review</b>	<b>13</b>
<b>2.1 Anatomy of the breast Structure</b>	<b>13</b>
<b>2.2 Causes of Implications towards breast implant</b>	<b>14</b>
2.2.2 Causes for infections	15
2.2.3 Causes for rupture	15
<b>2.3 Critical forces subjecting the breast structure</b>	<b>16</b>
<b>2.4 Application of Finite Element Methods in Material Testing</b>	<b>17</b>
<b>2.5 Comparison of New Materials Trends in Breast Implant</b>	<b>18</b>
<b>2.6 ANSYS</b>	<b>19</b>
<b>3.0 Research Objectives</b>	<b>21</b>
<b>4.0 Project description</b>	<b>23</b>
<b>4.1 Key Methodology</b>	<b>23</b>
<b>4.2 Steps for Ansys Modelling</b>	<b>24</b>
4.2.3. Geometry Input	25
4.2.3.1 Geometry design with SCAD file	25
4.2.3.2 Solid Work Modelling	26
4.2.4 ANSYS Inputs	27
4.2.4.1 Selection of Geometry Part	28
4.2.4.2 Material Data Input	29
4.2.4.3 Definition of Initial Condition	30
4.2.4.4 Step Sizing	31
4.2.4.5 Mesh Analysis	32
4.2.4.5.1 Clarification on Mesh Quality	34
4.2.4.5.1.1 Skewness of Mesh	34
4.2.4.5.1.2 Jacobian Ratio of the Mesh	35
4.2.4.5.1.3 Orthogonal quality of mesh	36
4.2.4.6 Force Input	36
4.2.4.6.1 Force Input (I)-Modelling the Force formed through biofilm	37
4.2.4.6.2 Force Input (II)-Modelling the Hydrostatic Force (Body Submerged inside the liquid)	39
4.2.4.6.3 Force TYPE (III)-Fixed Support	39
<b>4.3 Interpretation of Results</b>	<b>40</b>
4.3.1 Interpretation of Deformation Change	41
4.3.2 Interpretation on directional velocity dissipation in breast implant	43
4.3.3 Analysis of stress intensity	44
4.3.4 Strain Energy	44
4.3.5 Maximum Shear Stress	45
4.3.6 Normal Elastic Strain	46
4.3.7 Interpretation of normal stress	47
4.3.8 Interpretation of velocity propagation	48
<b>4.4 Discussion</b>	<b>52</b>

4.4.1 Future Opportunities	52
4.4.2 Current Challenges	54
<b>5.0 Conclusions</b>	<b>56</b>
<b>6.0 Bibliography</b>	<b>57</b>
<b>7.0 Appendices</b>	<b>63</b>
Appendix A: Figures Related to Meshing Process	63
Appendix B: SCAD file source code to Design Breast Implant	67
Appendix C: Silicone Property Data	68
Appendix D: Material Property Options to be selected for Future Use	69
Appendix E: Theoretical Silicone Non-linear Stress Strain Curve	70
Appendix F: Step Sizing, Numerical Method Control, Damping Control, Visibility Management Options	71
Appendix G: Breast Size Chart Samples	73
Appendix H: Different ANSYS Modelling Suite	74

## **Lists of Tables**

Table 1 Compression Testing Results of the Cells.....	16
Table 2 Value of Skewness and Cell Quality (Ozen, 2014).....	65
Table 3 Wacker Silicone Material Properties and Standards .....	68
Table 4 Mooney-Reviling stress strain response of Silicone material to check the fatigue strength .....	71

## **List of Equations**

Equation 1 Initial velocity condition for breast implant .....	30
Equation 2 Initial acceleration condition for breast implant .....	30
Equation 3 Equation of Skewness .....	35
Equation 4 Equation for Jacobian Matrix .....	35
Equation 5 Dot product of area vector of face and vector from centroid of the cell to centroid of that face.....	36
Equation 6 Dot product between area vector and centroid of mesh cell to its adjacent.....	36
Equation 7 Equation of Stress Intensity.....	44

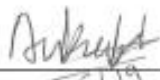
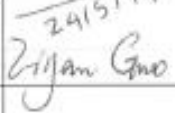



## **List of Figures**

Figure 1 A Anatomy of the breast B. Incision point of the breast .....	13
Figure 2 Work Flow Chart for ANSYS modelling of breast implant .....	23
Figure 3 SCAD breast model A: SCAD model B: SCAD model inputted inside space claim.....	25
Figure 4 Solid-Work Modelling (A): Top View, (B) Side View, (C) Bottom View and (D): Side View.....	26
Figure 5 A: Face Selection Method B: Body Selection Method C: Vertices Selection D: Wireframe Selection.....	28
Figure 6 Material Properties of Silicone .....	29
Figure 7 Time Step Input .....	31
Figure 8 Shell Element (Abacus 6.10, 2018) .....	32
Figure 9 Finite element mesh of 2D axisymmetric model of studied cylinder shown at $\frac{3}{4}$ circular expansion .....	32
Figure 10 Mesh Skewness Bottom View of the breast .....	34
Figure 11 Figures showing vector variables .....	36
Figure 12 Point Loaded Non-Uniform Transient Force Input.....	37

Figure 13 Hydrostatic force showing the loading and force direction .....	39
Figure 14 Fixed Support Structure .....	40
Figure 15 Deformation changes A: Bottom Area (Fixed Support) View, (B) Side Area (C) Top Area .....	42
Figure 16 Acceleration in 2sec is going upward at 7 second going downward 14 second upward again.....	43
Figure 17 Graph for acceleration.....	43
Figure 18 Stress Intensity.....	44
Figure 19 Strain Energy.....	45
Figure 20 Maximum Shear Stress.....	46
Figure 21 Normal Elastic Strain .....	47
Figure 22 Normal Stress Acting on the Implant.....	48
Figure 23 the velocity propagation.....	49
Figure 24 Cyclic Stress Curve generated using the fatigue strength coefficient ..	50
Figure 25 Duty Cycle of the breast implant under subjected load and material properties. ....	50
Figure 26 Curve for Speculative and Critical Design (Johannessen, n.d.).....	52
Figure 27: Mesh Properties Table Data.....	63
Figure 28 Mesh Solving Status.....	64
Figure 29 Meshed Breast .....	64
Figure 30 Relationship between Colours of the mesh and mesh quality (Ozen, 2014) .....	65
Figure 31 Mesh Skewness Size Distribution of our designed breast implant .....	66
Figure 32 Scad File Source CODE.....	67
Figure 33 Material data input screenshot 2 .....	69
Figure 34 Material Data input option screenshot-1 .....	69
Figure 35 Engineering Data and ANSYS product Suite .....	70
Figure 36 Neo Hooke and Relationship of Elastomer.....	70
Figure 37 Uniaxial biaxial and shear curve of Silicone Material.....	71
Figure 38 Step Size Number .....	71
Figure 39 Directional Deformation for 10 steps Transient force.....	72
Figure 40 Stress Intensity of the breast.....	72
Figure 41 Breast Size Chart Examples.....	73
Figure 42 ANSYS Product suite .....	74



## Contribution Table

NAME	Student IDs	Percentage of Effort Added by Team Member	Justifiable Mark Award out of full mark of the assignment	Signature.
Ar kar Nyan Hein	N8709041	38%	100%	
Ziyan Guo	N10054553	14%	100%	 24/5/19 Ziyan Guo
Hamza Nazir Malik	N10240420	14%	100%	
Yichen Hsu	N9806733	14%	100%	
Naveen Paruchuri	N10327894	14%	100%	 24/05/19
Bhavin Jieshbhai Vyas	N10017518	1-2%	50%	—
Keyur Kanubhai Patel	N10176896	1-2%	50%	—





## Executive Summary

This report initially explored the materials and challenges related to the breast implant. Some of the material studied in this report include Nano-composite materials (Nano-diamond, Nano-gold and Nanosilver to be used on breast implant). Moreover, polyurethane, polysiloxane and silicone rubber were compared and contrasted as in literature review sections.

After that, the report highlighted the key challenges associated with mastectomy procedures which involve infection related difficulties, rupture and vascular contracture.

After the literature review, the challenge topic of vascular contracture was chosen. Then, a novel simulation procedure was developed to tackle the challenge as it is the most accessible way for the team to achieve a meaningful solution outcome for the time being.

This procedure includes applying ANSYS modelling software integrated with solid work and SCAD to solve transient and non-uniform external forces acting toward the breast implant geometry.

As for the model being used, the implant model was designed to be a simplistic model or baseline model rather than the realistic model. However, the model can be easily adjusted based on material properties requirement, the force distribution pattern of bacterial adhesion, position magnitude and type of forces, required mesh size and geometry to reflect the realistic nature of the implant model.

The key results and findings include the production of the graphical and numerical solutions of transient and non-uniform directional deformation, directional acceleration, distribution of stress intensity, normal elastic strain, normal-stress, velocity changes corresponding to the forces exerted on the implant. As the per result prediction, most of the stress and directional acceleration pattern correspond to the force we have inputted in the ANSYS modeller.

Additionally, fatigue strength and duty cycle of the implant were calculated by using the cyclic stress-strain graph generated from possible factors. The factors are required to be justified based on the nature of the material being used.

After the results were predicted, limitation and accuracy of the design, future development opportunities and challenges were discussed. The scale-up research opportunities are also discussed in this report.

## 1.0 Introduction

In this society, the high significance is placed on the physical appearance of both genders. As for the male, ideal height and weight are highly emphasised. According to the study done by Jackson and Ervin, female perceived male's height to be directly proportional to social attractiveness, professional status, and masculinity and inversely proportional to femineity (Jackson & Ervin, 1992). Similarly, according to American garment industrial standards, size 4 (hips), size two waist and size ten bust woman are portrayed as the sexual ideal, the mirage and the fantasy to general woman population. Even so, this non-existent perfect figure is used by a woman as a point of reference to improve their self-images (Harrison, 2003).

Amidst the attraction conformity, augmented mastectomy has taken the significant market share of those standards. According to global Market Insight, the US breast implant market alone for Silicone implant is about USD 700 million in 2018 and is expected to reach up to 1.2 billion dollars by 2025. As for the Asia Pacific market, Australia is ranked in 4<sup>th</sup> place preceded by India, Japan and China (Global Market Insight, 2019). By analysing this market further, cosmetic breast augmentation market has taken 85% of the market shares (Global Market Insight, 2019). Additionally, the breast augmentation market has increased for 548% over a decade (i.e. from the 1990s up to 2005) while the average implant size has increased for 40% over a decade (Goodman & Walsh Childers, 2004).

Unsurprisingly, the underlying psychological driver to this exploding market data complies with the experiment conducted by Harrison. According to Harrison, the study was conducted at large Midwestern University at Illinois with 18-25 age group with mostly Caucasian 149 females and 89 males. The results of the study show that the average woman's ideal breast is 1.02 larger than their actual breast. Meanwhile, Men's ideal breast size for a woman is 2.09 larger than a woman's actual breast (Harrison, 2003). Similar studies are also done by Dunn and Thompson, where 55% of the woman long for larger breast (Dunn & J.K., 2000). Furthermore, the studies done by Goodman has also shown

that 34% dislike their breast and 91% of those are willing to undergo augmentative mastectomy or reduction surgery to achieve C cup size ten as bombarded by media (Goodman & Walsh Childers, 2004).

Although the ladies tried to overcome this dismal objectionable social expectation by taking breast augmentative surgery, the procedures for this surgery come at a high price. These include increasing the risk of rippling of the breast, breakage, microleakage, immune disorders, cancer such as T-cell hyperplasia, Anaplastic large cell lymphoma (HU , et al., 2015), symmastia, mal-positioning, unnatural feel (Baxter, 2003). Moreover, there are infectious bacteria from various sources such as *S. Aureus*, methicillin-resistant *Staphylococcus* spp. In some cases, rare infections from exposure of Brucella, Streptomyces from the soil and Pasteurella *multocida* infection from a pet can be developed (Song & Ooi, 2016). Other fungal infections, such as mycobacteria and yeast infection, are also prevalent. These infections, in turn, cause aesthetic distortion, pain and distress to the patient. Moreover, the development of biofilm can cause the swelling of large cell lymphoma. (Song & Ooi, 2016). All these challenges mentioned are the medical related implication, and psychological difficulties are not addressed due to the scope of this report.

To address all the challenges and material innovation related to breast implant is very far beyond the scope of this report and may require the years of studies from a multitude of experts.

**Therefore, this report aims to narrow down the focus to create the simplistic breast model, describing the stress propagation to predict the vascular contracture. This model tries to achieve the basic functionality of stress propagation and deformation analysis based on existing theories.**

## 2.0 Literature review

### 2.1 Anatomy of the breast Structure

Before studying the critical forces acting the breast, it is crucial for the team to understand the underlying anatomy of the breast. The anatomy of the breast is as shown in Figure 1 A while the incision points are as shown in Figure 1 B). The very detail description of the anatomical parts of the breast will not be described due to the limited nature of this report. The anatomy structure is outlined as they are incredibly crucial in understanding implant placement and forces exerting towards the implant for further finite element method analysis. For example, choice implant placement between sub-granular and sub-pectoral can be critical factors for the cause of rippling, palpability, increased capsular contracture and scar tissue formation which will play a vital role in modelling process of the future.

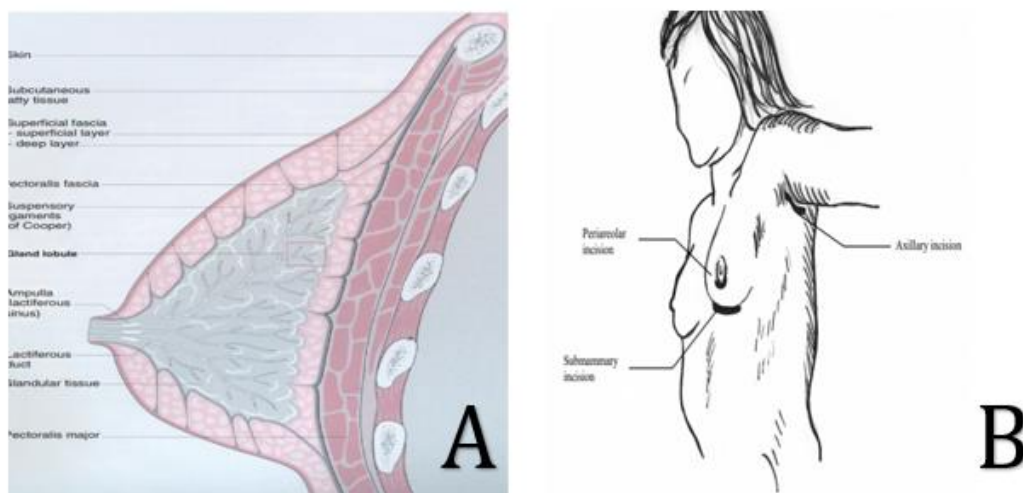


Figure 1 A Anatomy of the breast B. Incision point of the breast

## 2.2 Causes of Implications towards breast implant

Literature review of causes of implication towards breast implant was made to generate new ideas to solve these implication challenges.

### 2.2.1 Causes for capsular contracture

Like any other surgery, breast implant surgery is also linked with several risks and complications. Capsular contracture is one of the most common post-implant complications and one of the most common factors leading to the second surgery. Capsular contracture is an inflammatory reaction of the human body's immune system against the entering foreign material. (Headon, Kasem and Mokbel 2015). Many types of research are ongoing to identify the possible causative factors of capsular contracture. The current idea is that there are multiple factors combined cause the capsular contracture to occur. These factors include bacteria, tissue trauma, and blood, implant type, and inflammation due to surgical techniques. These sums together to cause capsular contracture (Tamboto, et al., 2010). However, the reason for capsular contracture on breast implants remains uncertain. The primary concept is that a clinical infection around the implant plays a role in the growth of capsular contractions. Recent researches show the capsular contracture is associated with a clinical disease while other researchers have found links between the presence of bacteria and the occurrence of capsular contraction. However, the origin of the bacteria is not clear (William P. Adams Jr 2009), (Yara Bachour 2019).

### 2.2.2 Causes for infections

Breast surgeries and augmentation comes with a high risk of diseases. Infection rates among reconstruction procedures are significantly higher than primary breast augmentation surgeries. Implant-related infections occur in around 35% of reconstruction after mastectomy and from 1.1% up to 2.5% of augmentation procedures. (Tahaniyat Lalani MBBS 2018). Infections are on the top of the complications which occur after the breast implant surgeries. Bacteria find their way into the surgery site and the host regardless of how careful the surgery has been attempted. Six contributing bacteria that are primarily involved in implant-related infections: *Staphylococcus epidermidis*, *S. aureus*, *Escherichia coli*, *Pseudomonas aeruginosa*, *Propionibacterium*, and *Corynebacterium* (Prasad, et al., 2019).

Additionally, recent data indicated that *Serratia*, *Enterococcus*, *Enterobacter*, group (B) *Streptococcus*, and *Morganella* have also been associated with the reconstructive population (Pittet, Montandon and Pittet 2005).

### 2.2.3 Causes for the rupture

Rupture of the breast implant can occur through a pinhole-sized hole or a visible large scar or tear. This tear can also lead to the bleeding of silicone oil from the silicone envelope. The published work identifies several reasons for a breast implant, but no many are due to trauma. A few identified causes of implant rupture are 1) Weak or aged silicone envelope or shell; 2) Manual compression during mammography; 3) Trauma from fall, accident, wound and gunshot have been reported so far. However, the age of the implant remains the most common factor resulting in implant rupture (Hillard, et al., 2017). Researches on the rupture of the implant concerning the years after implantation suggest that after eight years of initial implantation, the implant may either be removed or replaced (Handel N, et al., 2013).

## 2.3 Critical forces subjecting the breast structure

To find out the critical forces acting on the breast structure remains the significant challenges due to the geometrical irregularities, difficulty in cut intact, test sample sizing and tissue damage during the gripping process. Moreover, different physiological factors impose significant challenge in determining critical forces acting on the implant.

Other critical forces under hypothesis include forces from pectoral muscle, forces from bacterial adhesion, osmotic pressure and hydrostatic force within and surrounding part of the implant.

The bacterial biofilm effect on breast structure may be evaluated using an elastic theory, which is linear elastic theory, neo-Hookean relations and non-linear inverse elasticity theory (Goenezen, et al., 2012).

To understand fully on these theories are beyond the scope of the report. However, the validation methods to test the mechanical properties of cells are mentioned in section (4.4.1 Future Opportunities).

At this stage, some of the biomechanical forces of fat tissue and surrounding cells, as shown in table (1) to understand them in the future modelling process.

**Table 1 Compression Testing Results of the Cells**

Lead Author	Experimental Condition	Constitutive Model	Fat Stiffness	Fibroglandular Tissue Stiffness	Tumor Stiffness
Nellman et al. <sup>44</sup>	<i>Ex vivo</i> punch indentation	Linear elastic and exponential relations	$E = 17.4 \pm 8.4$ kPa at 15 % strain	$E = 271.8 \pm 167.7$ kPa at 15% strain	$E = 2162$ kPa for ductal carcinoma <i>in situ</i> (DCIS)
Krouskop et al. <sup>43</sup>	<i>Ex vivo</i> compression loading	Linear elastic relation	$E = 20 \pm 8$ kPa at 20% compression	$E = 48 \pm 15$ kPa at 20% compression	$E = 290 \pm 67$ kPa for DCIS
Del Palomar et al. <sup>21</sup>	<i>In vivo</i> gravity loading	Neo-Hookean relation	$C_1 = 3$ kPa	$C_1 = 12$ kPa	N/A
Samani et al. <sup>42,46,47</sup>	<i>Ex vivo</i> compression loading	Linear elastic model and polynomial functions	$E = 3.25 \pm 0.9$ kPa at 5% compression.	$E = 3.24 \pm 0.61$ kPa at 5% compression	$E = 16.38 \pm 1.55$ kPa for DCIS
Rajagopal et al. <sup>24</sup>	<i>In vivo</i> gravity loading	Neo-Hookean relation	$C_1 = 0.08$ , and 0.13 kPa for two volunteers	$C_1 = 0.08$ kPa, and 0.13 kPa for two volunteers	N/A

(Nielsen, et al., 2009)



## 2.4 Application of Finite Element Methods in Material Testing

Application of Finite Element Methods is reviewed to emphasise the importance of FEM in biomedical implant prototype development.

FEA is beneficial to any project which demands the understanding of strength, durability and dynamics of materials.

By Using sophisticated software tools including Nastran, Abaqus or ANSYS, one can simulate the interaction and movement among components in the system, given a set of boundary conditions and material properties (Element, 2018).

With innovative new materials emerging in bio-medical industries during the era of industry 4.0 (Lee, et al., 2015) , it is expected that application of FEA tools will play the critical role in understanding the mechanical, thermal and shape memory effect of newly discovered material during the prototyping processes (Parthasarathy, et al., 2011) (E, et al., 2013).

In general, Finite Element Modelling can:

- Assess the performance of the prototype made with newly discovered material (PERUSIC, 2017)
- Identify the faults associated with new material properties before commercialisation process begin (PERUSIC, 2017)
- Avoid trial and error approach (PERUSIC, 2017) during the manufacturing of products using the novel material.

## 2.5 Comparison of New Materials Trends in Breast Implant

Breast implants filled in with silicone-gel and covered with polyurethane foam were introduced in the 1970s. These types of implants were used by 110,000 women in America (Handel, 2006). However, as there were concerns that this material is toxic, it was banned in the US. This kind of implants are still being used in many countries around the world (Handel, 2006). The occurrence of capsular contracture was quite low for implants covered with polyurethane foam when compared with textured or smooth implants. There were not many complications related to polyurethane implants other than a transient skin rash (Handel, 2006). It was found that the chances of occurring of capsular contraction and the amount of polyurethane coating on the implant are inversely related (Castel, et al., 2015). Decreased amount of polyurethane coating on the implant's surface, was associated with severe capsular contracture (Castel, et al., 2015). According to (Handel, 2006) the safety profile of implants covered with polyurethane foam is similar to that of silicone filled implants, and the risk of long term capsular contracture is reduced as a result of polyurethane coating (Macdonald, et al., 1995).

Polysiloxanes or silicones, which are the main constituents in breast implants, are chemically inert in general. However, there is a chance of developing autoimmune connective tissue disease due to immunological sensitisation to silicone (Macdonald, et al., 1995) (Brook, 2006).

Platinum is used as a catalyst to crosslink silicones using hydro-silylation reaction (Brook, 2006). Studies have been conducted on the amount of platinum that bleeds from these implants. As a result of the study, it was found that platinum in silicon-based implants is linked with highly toxic and unusually high oxidation state (Brook, 2006).

The complications that were found out with breast implants injected with Polyacrylamide gel are a hematoma, persistent mastodynia, abnormal skin sensations, multiple induration and lumps, inflammation and unsatisfactory contour results (Cheng, et al., 2002).

## 2.6 ANSYS

Before modelling process about ANSYS is introduced, the brief review on ANSYS is made to understand the capability of ANSYS in material science

Preceding to a discussion about ANSYS, it is crucial to review the fundamental theories behind ANSYS to explore why ANSYS is applied in material science.

The review begins with understanding the definition of validation and verification of models in engineering designs. Model verification is defined as “ensuring that the computer program of the computerised model and its implementations are correct” (Sargent, 2004). Meanwhile, model validation is defined as *“substantiation that a computerised model within its domain of applicability possesses a satisfactory range of accuracy consistent with the intended application of the model”* (Schlesinger, 1979). From this definition, it is very imperative to note that verification without validation is simply the “pretty diagram” and validation without verification is *“simply the waste of time and energy”*. Therefore, before validating the new material in real-world ANSYS should be used to model the prototype using novel material before the material is placed in the commercial market.

Now, as the vital part of this topic, we would like to review what ANSYS does why ANSYS is used. ANSYS focus on engineering simulation with 45 years of simulation portfolio. ANSYS advances and devises engineering simulation software (ANSYS Inc, 2015).

ANSYS has a long reputation for verification aspect of software modelling in various engineering designs from different industrial products including but not limited to defence vehicles and products (i.e. rockets, jets, missiles and bullets), medical implants, building infrastructure and process equipment.

As for the ANSYS portfolio, ANSYS is also used in many different well-known industries. For example, many renowned defence industries such as Lockheed Martin Skunk Work (ANSYS, 2018) , Boeing Phantom Works (A Berkshire Hathaway Company, 2008), Pratt and Whitney (Pietzak, 2019), Raytheon (ANSYS Inc, 2015) consider the use of ANSYS as one of the mission-critical strategies.

Similarly, the use of ANSYS is adopted by Australian process industries and scientific institution including SRI (Sugar Research Institute), Commonwealth Science and Industry Research Organization (CSIRO), SHELL, GLENCORE, Tesla to name few among a countless number of organisations.

As for this breast implant modelling project, ANSYS can be used for modelling in-conjunction with MRI data and to explore the application of novel implant material properties, non-linear material modelling (Nielsen, et al., 2009), hyperelasticity (Garbey, et al., 2014), viscoelasticity, pore pressure and shape memory (Weems, et al., 2017), non-linear contact modelling, parametric analysis of implants and fatigue calculations over time.

### 3.0 Research Objectives

There are not many papers modelling the breast implant structure using modelling software. Additionally, there are not many transient force analysis models specifically related to the breast implant except few articles. In this paper, we have divided our research objectives into three categories. These include (i) one current achievable research target, (ii) scale up objective and (iii) commercial purpose.

**The current research objective is** to design the simplistic and theoretical transient stress model of breast implant by applying a combination of Solid-Work, SCAD and ANSYS software using the traditional silicone material properties data.

**The scale-up objectives are:**

- To improve the mesh of the breast implant.
- To compare and contrast the stress propagation and deformation of breast-implant by simulating with different materials while keeping the other variables under steady and uniform conditions.
- To simulate stress propagation responding to different compression, shear force and buckling load while keeping the material properties, initial conditions and mesh geometrical properties as constant.
- To test the implant under different initial condition while keeping the other parameters fixed.

**The final commercial scale-up concept and vision of this project are:**

- To create the replica of a simulating environment between bio-implant and physiological environment. The simulation environment will ensure that less trial and error approach and implant wastage during the project lifecycle of manufacturing and R & D processes (ANSYS Advantage Staff, 2012).
- To Create the digital twin (Boschert & Rosen , 2016) of the breast implant by weaving and integrating it with augmented reality (AR) for human user

simulation interface (Schoroeder, et al., 2016), integration of genetic algorithm and swarm intelligence to Eulerian and Lagrangian modelling (Chen & Wang, 2002)for bacterial dispersion theory and force of biofilm, MRI data for optimized meshing (Samani, et al., 2001) and distributed & elastic cloud computing for computational effectiveness (Behr & Tezduyar, 1992) 😊😊 . The designed digital twin will improve the user comfort and sales experience before breast implant is placed.

## 4.0 Project description

### 4.1 Key Methodology

The modelling steps for the breast implant can be divided into two key phases. These include geometrical drawing phase and ANSYS design phase.

The geometrical drawing phase consists application of SCAD file and SOLIDWORKS to draw the desired geometry of the breast based on breast size chart or MRI data or randomly selected input. The same drawing can also be done in ANSYS space-claim (Lee, 2018) instead of using other software.

Meanwhile, analysing phase in ANSYS encompasses decisions related to the type of materials and material properties to be used, creation of optimum mesh geometry, setting up the initial condition, choices of the kind of force to be used and the solution to be generated.

Figure 2 shows the summary workflow chart was conceptualised to model the breast implant

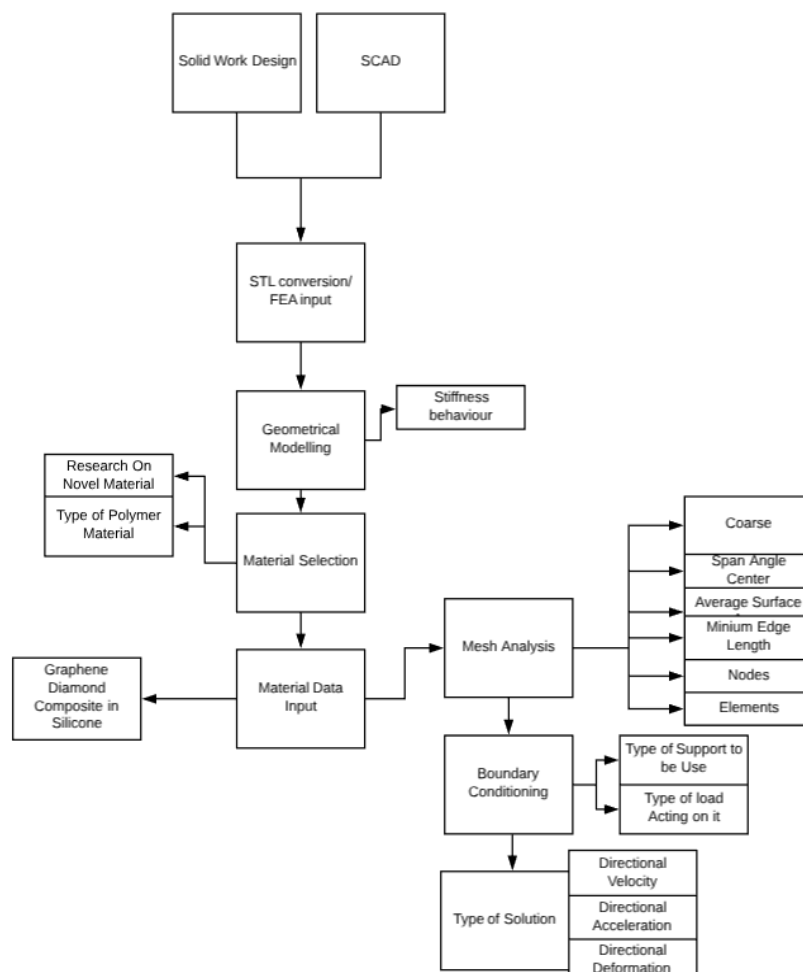


Figure 2 Work Flow Chart for ANSYS modelling of breast implant

## 4.2 Steps for Ansys Modelling

To clarify further on what has been described above the ANSYS modelling process is divided into eight methods. These include

1. Geometry Input
2. Defining Engineering Data (i.e. Material Properties Input)
3. Mesh Sizing
4. Establishing Initial Conditions
5. Analysis Setting which involves step sizing for transient forces, time interval of steps required, unit set up, selection of numerical method
6. Definition of external independent forces
7. Defining the solution outcomes needed for the analysis
8. Prediction of results

Further details relating to this process are described in the following sections.

Step (1) to Step (6) deals with the methodology section of this report while step (7) to step (8) deals with the results section of this report. The sections below will explain more in-depth on each level described in this section.



#### 4.2.3. Geometry Input

In the following sections (i.e. 4.2.3.1 Geometry design with SCAD file & 4.2.3.2 Solid Work Modelling ), geometrical modelling techniques associated with breast implant will be discussed.

##### 4.2.3.1 Geometry design with SCAD file

SCAD is the open source software used for designing 3D geometrical model. Unlike Solid-Work, it is not the interactive modeller but rather contains embedded interactive 3D compiler reading SCAD script code to generate the 3D model (Kintel, 2019). The system includes the variables and vector position, which allows the user to change the shape and size of breast implant as per dimensional breast requirement at relative ease (Kintel, 2019).

Detail scripts are described in Appendix (A) figure 23. The source codes are written by open sourced git-hub developers and breast implant researchers. After that, the breast implant diagram is generated, using the source code, as shown in Figure 3 (A).

The designed SCAD file is then converted into an STL file. The converted STL file is imported into ANSYS space-claim, as shown in Figure 3 (B), which can be edited for further meshing as required.

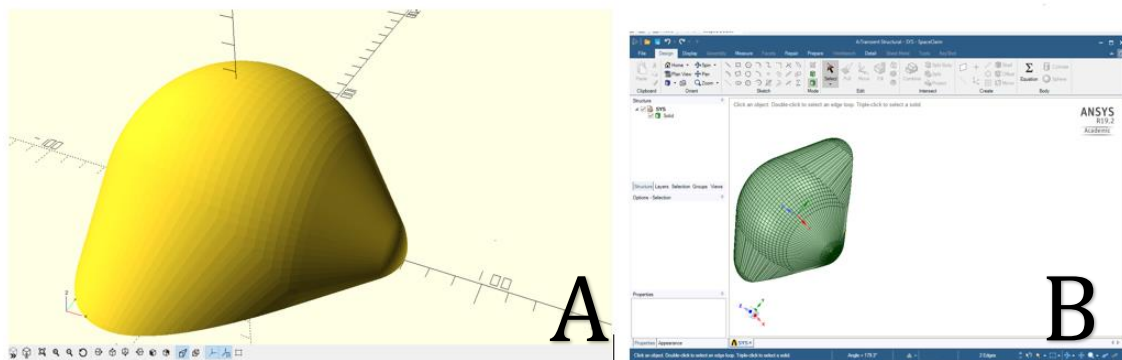


**Figure 3 SCAD breast model A: SCAD model B: SCAD model inputted inside space claim**

#### 4.2.3.2 Solid Work Modelling

The additional design method; solid work modelling, as shown in Figure 4, was also designed for a breast implant to input into ANSYS. This solid work model was developed using the arbitrary breast size chart data to demonstrate how easy it can be modelled. In this case, the width used here is 100cm with a height of 35 cm using an angle of curvature of 35 degrees. These values can be adjusted as per user requirement (i.e. breast size chart). The flexible geometrical designs from chart data can be further inputted into ANSYS as STL file for further finite element analysis.

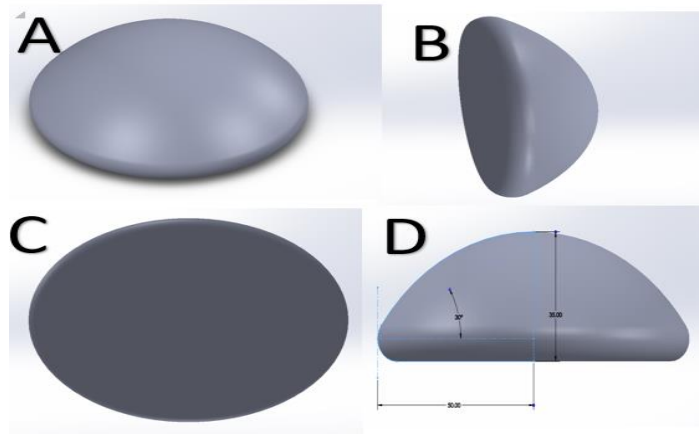


Figure 4 Solid-Work Modelling (A): Top View, (B) Side View, (C) Bottom View and (D): Side View

#### 4.2.4 ANSYS Inputs

The following subsections of this report deal with all the input parameters associated with ANSYS to carry out the transient and non-uniform stress analysis of a breast implant.

First of all, section (4.2.4.1 Selection of Geometry Part) will discuss the selection of geometry part, which is rudimentary techniques required for meshing and force input. After this, the report outlines how to enter silicone material data properties relevant to our design purpose as shown in (4.2.4.2 Material Data Input) and then the initial condition requirement as in (4.2.4.3 Definition of Initial condition)

After that technique relating to step sizing will demonstrate the transient nature of force as in (4.2.4.4 Step Sizing), then details of mesh parameters will be outlined, and procedures on how to check the good mesh are written in (4.2.4.5 Mesh Analysis).

Finally, this report will outline the justification of theoretical forces exerting on the breast implant to simulate stress propagation and deformation as in (4.2.4.6 Force Input).

#### 4.2.4.1 Selection of Geometry Part

Understanding how to select the geometry face in ANSYS is very imperative to analyse the force structure. By choosing the correct position of geometry, one can efficiently and realistically select the right mesh position to enter the force values efficiently.

Figure 5 demonstrates (A) Face selection, (B) body selection, (C) vertices selection, (D) wireframe selection of the breast implant. As for this project, a combination of random vertices and wire selection techniques were used for bacterial adhesion modelling while the face selection method was deployed for hydrostatic modelling.

The current selection for this project may not represent the realistic model. The geometry selection may become more realistic as we gather more information on bacterial dispersion model using either Eulerian (Neuman, 1984) or Lagrangian methods (Stohi, et al., 2005).

These methods may be integrated with artificial intelligence using a genetic algorithm (Haupt, 2005) and swarm algorithm (Schutte, et al., 2004) to predict data for microbial dispersion on breast using the initial conditions of bacteria growth.

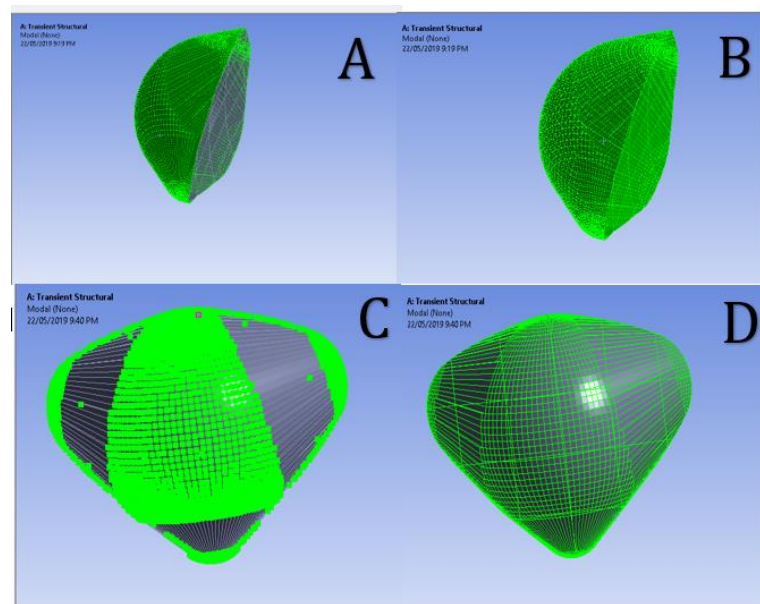
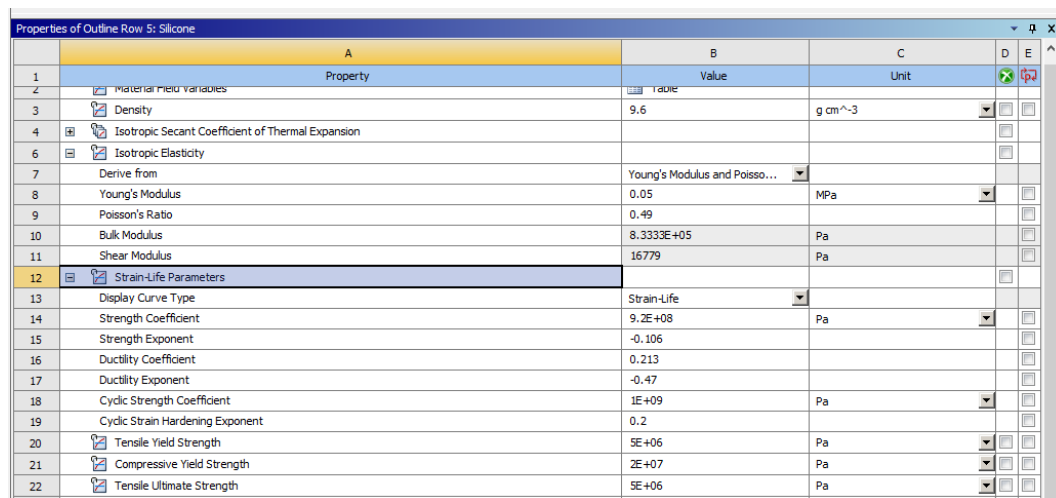


**Figure 5 A: Face Selection Method B: Body Selection Method C: Vertices Selection D: Wireframe Selection**

#### 4.2.4.2 Material Data Input

The second step for ANSYS input involves entering material data of Silicone for further analysis, as shown in Figure 6. In the case of transient force analysis, the properties of the critical material inserted are related to the strength of materials. These include Young Modulus, Poisson's Ratio, Bulk Modulus and Shear Modulus which calculate the Isotropic Elasticity. Moreover, other strength parameters, including stress life parametric coefficients, tensile yield strength, and compressive yield strength, were also added into the material parameter. Different material properties can also be used as ANSYS input for a different type of analysis such as computational fluid dynamics, structural shape memory, creep and fracture as shown in Figure 33 & Figure 34 at (Appendix D: Material Property Options to be selected for Future Use).

The silicone data entered as in Figure 6 is for demonstration purpose only. The new data value may be entered into this table as new novel material composites which are deployed as in the case of Nano-diamond or graphene composite.



Properties of Outline Row 5: Silicone				
	A	B	C	D E
	Property	Value	Unit	
1	Material Model Variables			
2	Density	9.6	g cm <sup>-3</sup>	
3	Isotropic Secant Coefficient of Thermal Expansion			
4	Isotropic Elasticity			
5	Derive from	Young's Modulus and Poisso...		
6	Young's Modulus	0.05	MPa	
7	Poisson's Ratio	0.49		
8	Bulk Modulus	8.3333E+05	Pa	
9	Shear Modulus	16779	Pa	
10	Strain-Life Parameters			
11	Display Curve Type	Strain-Life		
12	Strength Coefficient	9.2E+08	Pa	
13	Strength Exponent	-0.106		
14	Ductility Coefficient	0.213		
15	Ductility Exponent	-0.47		
16	Cyclic Strength Coefficient	1E+09	Pa	
17	Cyclic Strain Hardening Exponent	0.2		
18	Tensile Yield Strength	5E+06	Pa	
19	Compressive Yield Strength	2E+07	Pa	
20	Tensile Ultimate Strength	5E+06	Pa	

Figure 6 Material Properties of Silicone

#### 4.2.4.3 Definition of Initial Condition

This section deals with the definition of initial condition to set up the boundary conditions.

Definition of the initial condition means how breast is dynamically performing before the analysis has begun. As for this case, we have assumed a breast implant to be in a stationary state as the implant is considered to be in a fixed position. In the case of a damaged moving implant, the initial condition may have velocity value, which is not part of the scope of this project.

For the stationary condition, we have assumed the initial velocity to be in either steady state or at rest as shown mathematically in Equation 1& Equation 2

##### Equation 1 Initial velocity condition for breast implant

$$\int_n^{\infty} \frac{dv}{dt} = C$$

##### Equation 2 Initial acceleration condition for breast implant

$$\int_n^{\infty} \frac{da}{dt} = C$$

The other assumption is to assume initial velocity and deformation of the breast is at rest (i.e.  $v=0$ ) therefore  $\frac{dv}{dt} = 0ms^{-2}$ .

The initial condition may be set based on the dynamic state of the breast that the patient has been imposed before the FEA operation begins.

#### 4.2.4.4 Step Sizing

This section will explain how we set the steps to analyse the time we need for simulation.

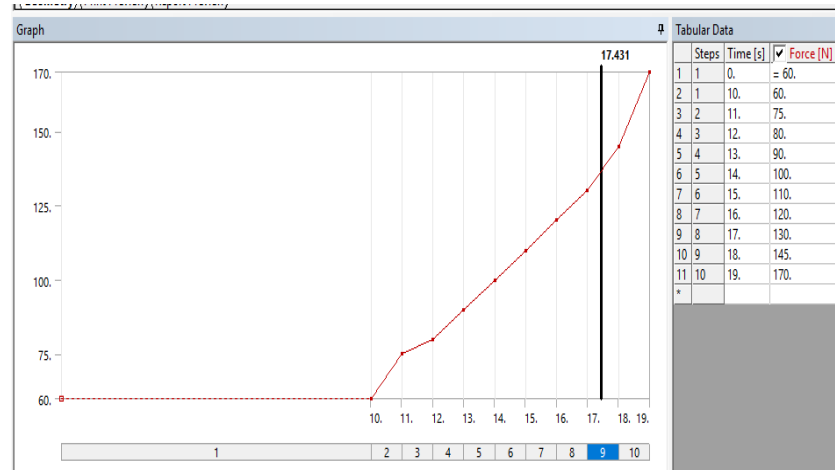
In the context of Transient force analysis of the breast, time step can be defined as *“time required for the shock wave to propagate through the smallest distance of the finite element of the breast”* (Avinash, 2018).

Time step sizing data may be retrieved based on the kinetic rate of the bacterial growth (Riesenberg, et al., 1991) and the stages of microbial growth on the breast (i.e. lag phase, log-phase, and stationary phase and death phase (Gardener, et al., 1998)).

For realistic modelling, it is suggested that time steps of minutes or hours instead of seconds should be used depending on the computing power availability. The bigger step size is favoured since the number of steps required for the solution is directly proportional to the required computing capacity.

As for this project, step numbers of 10 values are applied arbitrarily, as shown in

Figure 7. Between step 1 and step 2, as shown in Figure 7, the time of 10sec is assumed to demonstrate the lag phase of bacterial growth while other steps are considered to be in log phase. Detail step input options are as described in (Figure 38 Step Size Number) at (Appendix F: Step Sizing,



Numerical Method **Figure 7 Time Step Input**

Control, Damping

Control, Visibility Management Options).

After the inputted time steps, incremental forces of 60N, 60N, 75N, 80N, 90N, 100N, 110N, 120N, 130N, 145N, 170N were added. In a realistic model, bacterial bulk compression forces have to be added based on cytometry tests as described in section (4.4.1 Future Opportunities)

#### 4.2.4.5 Mesh Analysis

This section will explain how meshing is done and techniques on checking the quality of the meshes.

The mesh is then generated using the meshing tool provided by the Ansys, as shown in Figure 29 at (Appendix A: Figures Related to Meshing Process) while Figure 28 shows mesh solving status.

The meshing process provided here may not be reliable as we do not have required FEM expertise. The statement is supported by NASA technical fellow Raju who infamously quoted; “Not all beautiful colour plots are precise or accurate” (Dinel, 2017). The sources of mesh errors include the inability to identify loads and constraints acting on the breast structure, heavy reliance on auto meshing technique rather than generating the most suitable solid element for this breast implant purpose (Dinel, 2017).

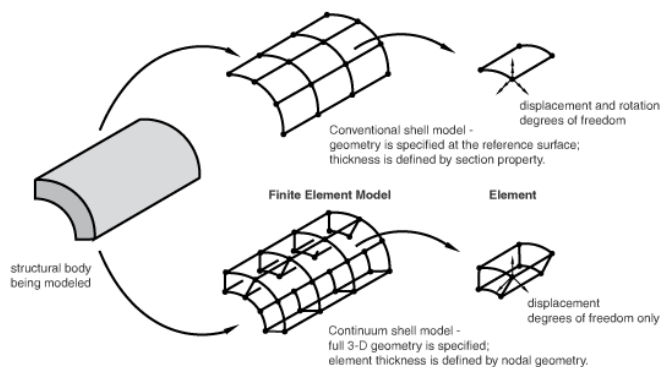


Figure 8 Shell Element (Abacus 6.10, 2018)

To overcome challenges to achieve the real-world mesh solution, discussions with experienced biomechanical engineers and FEA mathematicians are required to generate the detail fine meshing system. The discussion topics may include determining the number of mesh to be used, the convergence of the mesh and trade-off factors between computing capability and desired amount of meshes.

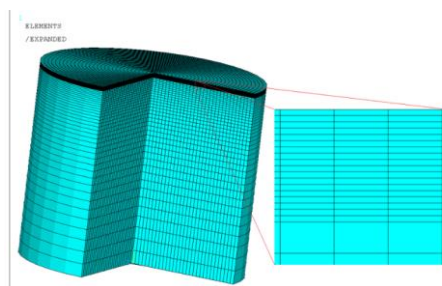


Figure 9 Finite element mesh of 2D axisymmetric model of studied cylinder shown at  $\frac{3}{4}$  circular

As for the project, the suitable mesh element geometry selected for breast implant is a capsule shape shell element, as shown in (Figure 8). This element is used since it is a curved structural element with the constant thickness (Wilson, 1999). Additionally, bodies of revolution under axially symmetric loading condition may



be used with the axisymmetric mesh as shown in (Figure 9 Finite element mesh of 2D axisymmetric model of studied cylinder shown at  $\frac{3}{4}$  circular expansion ).

#### 4.2.4.5.1 Clarification on Mesh Quality

This section outlines the input parameters used to generate this mesh geometry as well as techniques to check the quality of the mesh.

The details of the input parameters used for meshing are outlined in (Figure 27: Mesh Properties Table Data) under (Appendix A: Figures Related to Meshing Process). The quality of a mesh can be demonstrated in terms of skewness (Liu & Hwang, 2001), element quality, orthogonal quality and maximum corner angle. The following paragraphs will outline the key characteristics of mesh achieved for this project and theoretical meaning behind those properties, which are skewness, orthogonal and Jacobian ratio.

##### 4.2.4.5.1.1 Skewness of Mesh

This section explains the skewness of the mesh, which is one of the critical parameters in checking the mesh qualities.

The skewness of breast implant mesh is as shown in Figure 10.

According to Figure 10 & Figure 31 at Appendix A: Figures Related to Meshing Process, an average skewness achieved for this project is between 0.2-0.4, which proves that they are between excellent to sound quality. However, there are an insignificant amount of meshes with a skewness value of 0.8-0.9, which could be improved further.

The relation between the amount of skewness and cell quality is as shown in (Table 2 Value of Skewness and Cell Quality) & (Figure 30 Relationship between Colours of the mesh and mesh quality) to clarify further on achieved skewness value where skewness is defined as :

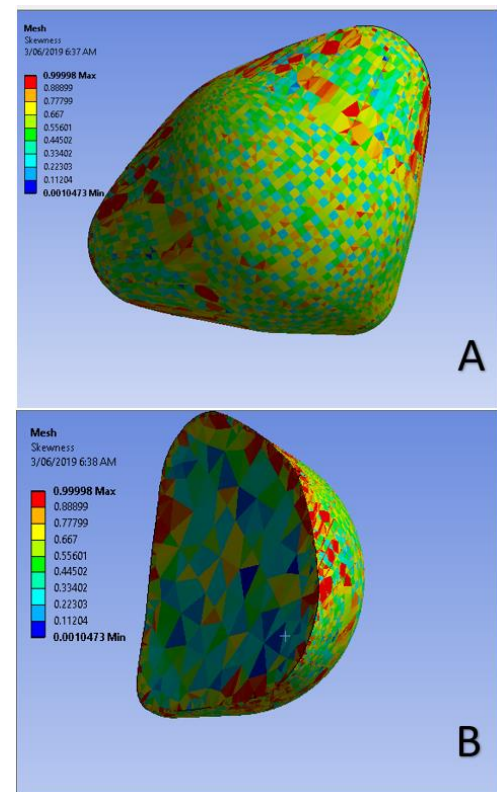


Figure 10 Mesh Skewness Bottom View of the breast

**Equation 3 Equation of Skewness**

$$Skewness = \frac{Optimal\ cell\ size - Cell\ Size}{Optimal\ Cell\ Size}$$

According to the equation, the value of 0 means perfect skewness is achieved while the number 1 implies the worst skewness result. This equation also means that ideally, our cell size has to be equal to the optimal cell size to achieve ideal skewness.

**4.2.4.5.1.2 Jacobian Ratio of the Mesh**

The second important parameter to determine the quality of the mesh is the Jacobian ratio. The Jacobian ratio can be defined as calibration of the geometry of the mesh element compared to that of the ideal or real element.

The Jacobian ratio, in general, improves the aspect ratio, wrapping factor and the control number of the meshes (Knupp, 1999). The mathematically Jacobian matrix can be defined as described in Equation 4.

**Equation 4 Equation for Jacobian Matrix**

$$J(\epsilon) = \frac{\partial F(x)}{\partial \epsilon}(\epsilon)$$

Where  $F(x)$  = modelling domain

$\epsilon$  = perfect element domain (Bucki, et al., 2011).

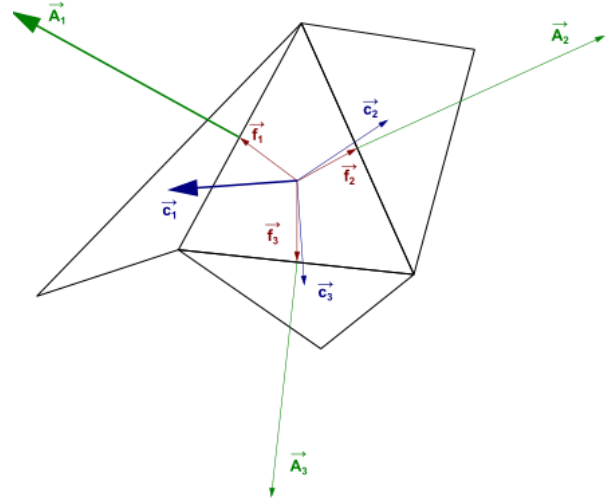
As for this project, we have a Jacobian ratio of corner node (Cianco, et al., 2007), the ratio used by Mechanical ANSYS Parametric Design Language (MAPDL) (i.e. the inverse of corner node) and Gauss point has an output value of 1. To clarify this number further, number 1 represents the highest quality mesh, while number -1 represents the lowest quality mesh.

Therefore, it is proven that the mesh generated for this project is the reasonable quality mesh according to the Jacobian ratio of the breast implant geometry.

#### 4.2.4.5.1.3 Orthogonal quality of the mesh

The ultimate way to measure mesh quality is by describing its orthogonality.

The orthogonality can be defined as “*area weighted average of angles between  $n$  and  $s$  vectors for all integration point surfaces of a control volume* (Tristan, 2018)”.



Orthogonality can be calculated using

Equation 5 and Equation 6, as shown on **Figure 11** Figures showing vector variables the following page.

**Equation 5** Dot product of area vector of the face and vector from the centroid of the cell to the centroid of that face

$$\frac{\vec{A}_i \cdot \vec{f}_i}{|\vec{A}_i| |\vec{f}_i|}$$

Where  $A_i$  = Area vector of face and  $f_i$  = centroid from the cell to face

**Equation 6** Dot product between area vector and centroid of mesh cell to its adjacent

$$\frac{\vec{A}_i \cdot \vec{c}_i}{|\vec{A}_i| |\vec{c}_i|}$$

Where  $c_i$  = centroid of cell to centroid of adjacent mesh cell sharing face

The definition of these symbols is also further clarified in Figure 11.

In general, orthogonality of zero is unacceptable while the orthogonality of 1 is of the best quality as described in Figure 30 at (Appendix A: Figures Related to Meshing Process). As for this project, we have achieved the orthogonality of 0.41845, which implies that it could be improved much further to make very fair quality. However, due to the time limit, we would like to improve this value in the next phase. 4.2.4.6 Force Input

#### 4.2.4.6.1 Force Input (I)-Modelling the Force formed through biofilm

As for the force input, 417 random mesh cells faces were randomly selected on the as shown in Figure 12.

The selection was made to demonstrate the non-uniform nature of the forces acting on the breast implant. (i.e.  $\frac{dF}{dA} = F(A)$ )

For the realistic solution, different amount of faces and different force magnitudes can be used based on the biofilm formation on the breast.

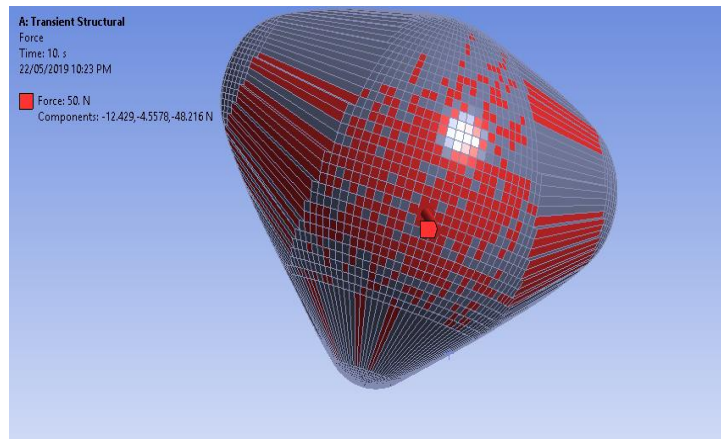


**Figure 12 Point Loaded Non-Uniform Transient Force Input**

According to the literature resource fatigue loading of 45N-450 N (S, et al., 2019) are used when testing the dental implants with bacterial adhesion forces. Dental implants do not reflect breast implants. However, once the similar in-vitro test is made for a breast implant, the data from those test can be used for future modelling predictions.

Additionally, it is imperative to note that different type of bacteria may contain a different kind of metabolic waste and different rate of biofilm formation and densities (Farshadzadeh, et al., 2018) (Dufrene, 2015) resulting in different non-uniform versatile loads. Therefore, contracture forces of bacteria on a breast implant may require extensive studies.

Finally, many non-uniform loadings by bacterial adhesion imply the need for massive computational power to build a realistic model. This may have to be overcome by the novel methods of numerical modelling technique which are better than conventional methods such as Hund's Rule (Anon., 1998), Newton Raphson method (Bruck, et al., 1989), Taylor Series (Foy, 1976), Euler's formula (Cryer & Tavernini, 1972) to name a few to optimize the numerical calculation performance algorithm by creating the simpler dispersion model algorithm.

High-performance computing, elastic cloud computing and distributed cloud calculations can be used to tackle this challenge, but this may require much energy as well as costs to perform the simulation.

#### 4.2.4.6.2 Force Input (II)-Modelling the Hydrostatic Force (Body Submerged inside the liquid)

As an additional requirement of the force input, Hydrostatic data is entered to breast implant assuming that breast implant may subject to hydrostatic pressure around the implant site which are fats and liquids (Quaini, et al., 2005) & (Cherrup, et al., 1989).

As for the data entry requirement of hydrostatic force, the direction of hydrostatic pressure, the density of Silicones and external pressure surrounding the implant were entered shown in Figure 13.

However, solutions relating to hydrostatic force cannot be analysed due to the data storage capacity of QUT lab computers. The running time has also increased with the increment of analysis query.

Therefore, the scope for analysing hydrostatics and hydrodynamics have been currently deleted from this project.

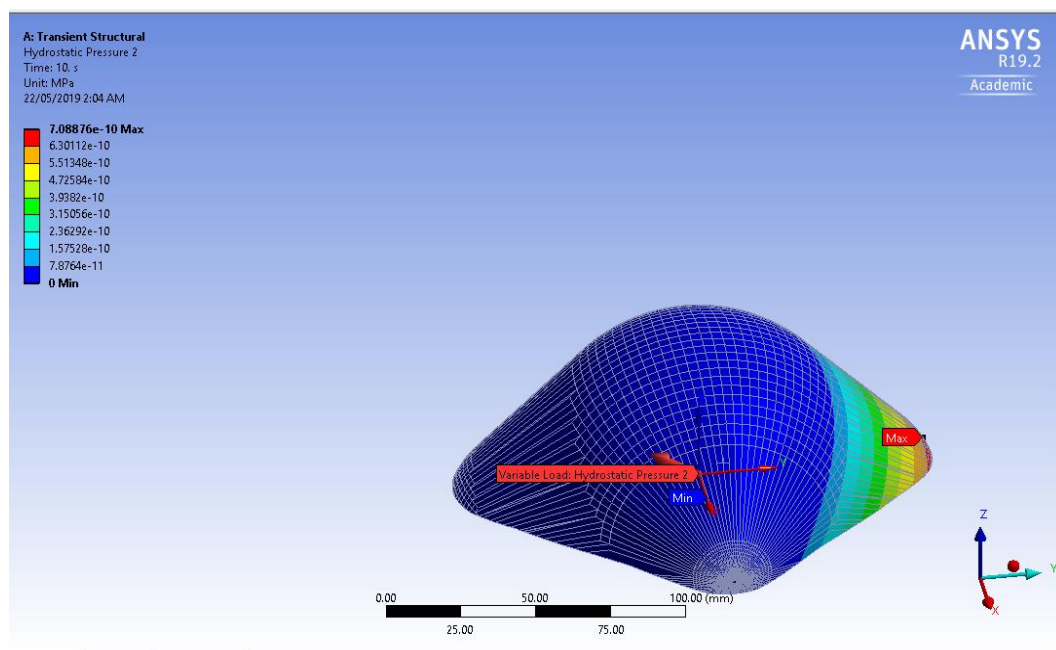


Figure 13 Hydrostatic force showing the loading and force direction

#### 4.2.4.6.3 Force TYPE (III)-Fixed Support

Finally, to get the solution fixed pin type support area was determined at the bottom of the implant, as shown in Figure 14.

The position was justified based on the assumption that a breast implant is fixed to the pectoralis major chest muscles supporting the breast implant. For the realistic model, the fixed support area should be justified based on the medical condition to be simulated on the breast implant.

Therefore, the boundary condition for a fixed area can be assumed as per the following equation again, since the breast is at rest according to the initial condition as already described in section (4.2.4.3 Definition of Initial Condition).

Therefore we could assume  $F, v, a=0$  in this fixed support area which can be interpreted mathematically as:

$$\int \frac{dF}{dt} = C$$

$$\int \frac{dv}{dt} = C \text{ms}^{-1}$$

$$\int \frac{da}{dt} = C \text{ms}^{-2}$$

It is also important to note that the fixed support area is the area where stresses are dissipated to zero as forces on the top and side of the breast are applied.

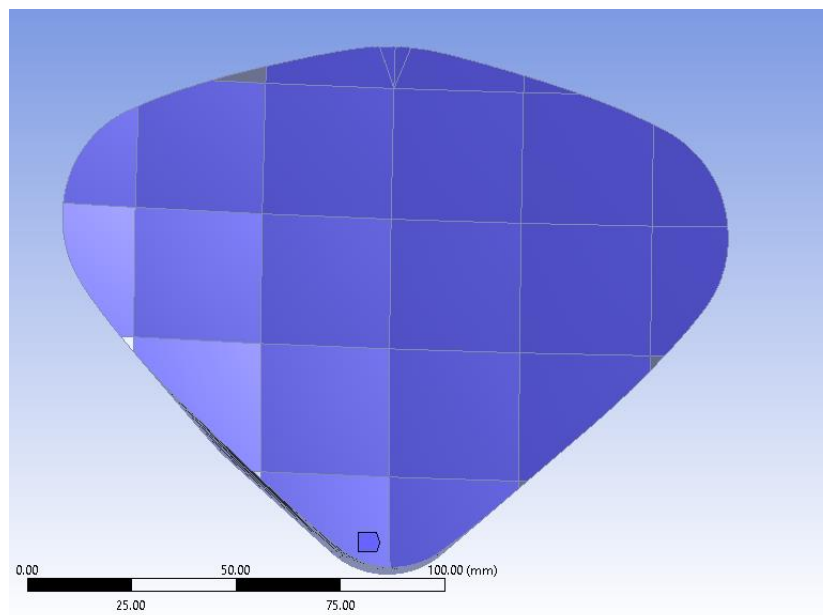


Figure 14 Fixed Support Structure



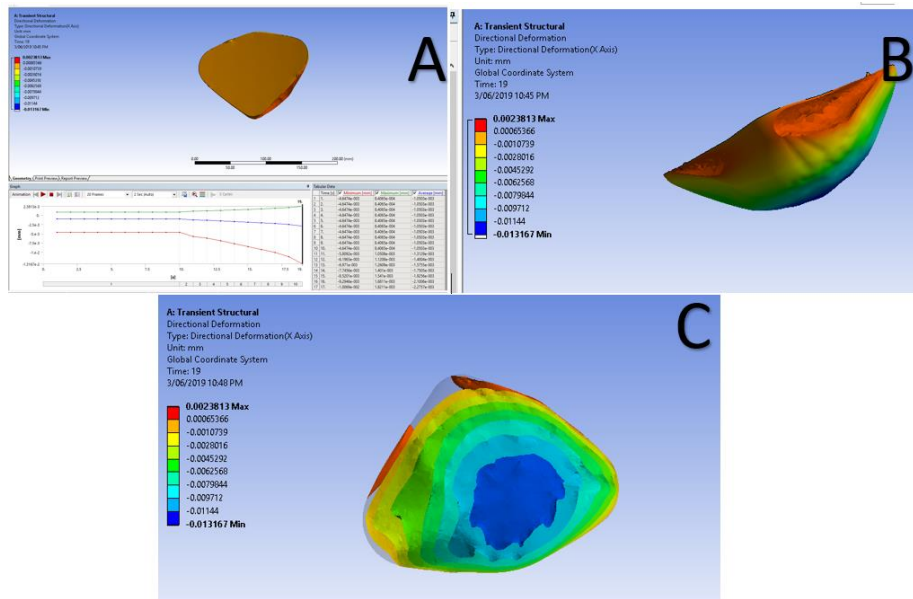
### 4.3 Interpretation of Results

Using the given set of input parameters as mentioned above, we have generated the solutions for stress propagation, strain and deformation shockwave propagation of the breast implant.

The sections below describe the directional deformation, direction of acceleration, stress intensity, strain energy, maximum shear stress, normal elastic strain, normal stress and equivalent elastic strain. Details and several figures are also described.

### 4.3.1 Interpretation of Deformation Change

**Figure 15 Deformation changes A: Bottom Area (Fixed Support) View, (B) Side Area (C) Top Area**



According to figure 15 (A) results, the directional deformation in the fixed support area was 0.000653, directing upward, which is the opposite direction the force input. Meanwhile, axial buckling deformation in sideways of the breast was observed with the value of 0.0024mm, as shown in

(B). Finally, the downward strain was found on the top of the breast with value of 0.014mm, and it gradually decreases as the stresses propagated near the fixed support structure, as shown in

(C). From this analysis, it is found out that the displacement values shown here correspond to the force that has been entered previously in (4.2.4.6.1 Force Input (I)-Modelling the Force formed through biofilm).

#### 4.3.2 Interpretation of directional velocity dissipation in breast implant

The directional acceleration of the breast was observed using acceleration propagation diagram as shown in Figure 16 as well as using the video file in the ANSYS software, which is available on request. According to the video file, the acceleration was moving downward as force is applied from the top of the breast. However, it is also observed that the acceleration of breast implant was directing upward since force are also exerted from the side of the breast, which has larger mesh area. This creates the squishing effect and damping of the breast due to the elastic nature of silicone.

Detail numerical value for acceleration shown in Figure 17 Includes the red area representing

$0.018 \frac{mm}{s^2}$  (upward direction), blue area in Figure 16 (B) representing  $0.017 \frac{mm}{s^2}$

(downward direction), green area in Figure 16 (C) showing  $0.00159 \frac{mm}{s^2}$  (downward direction). Additionally, the graph in Figure 17 has shown the sinusoidal curve showing the damping nature of the breast implant.

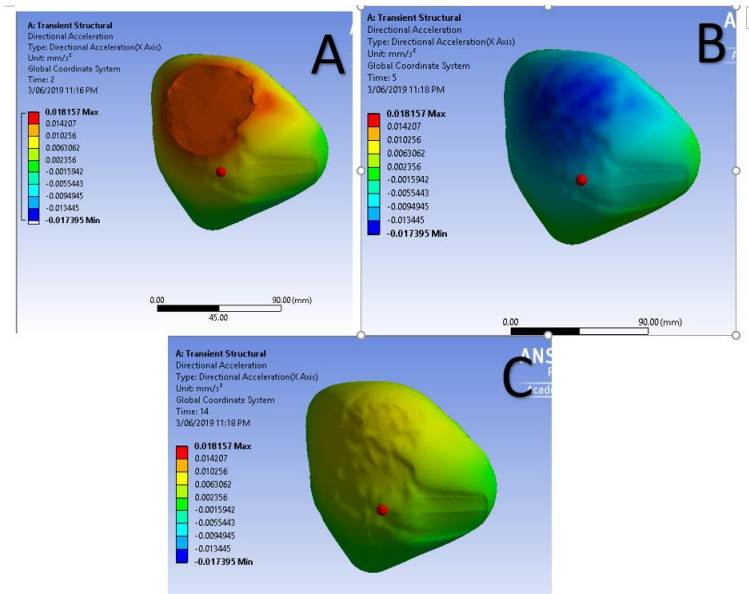


Figure 16 Acceleration in 2sec is going upward at 7 second going downward 14 second upward again

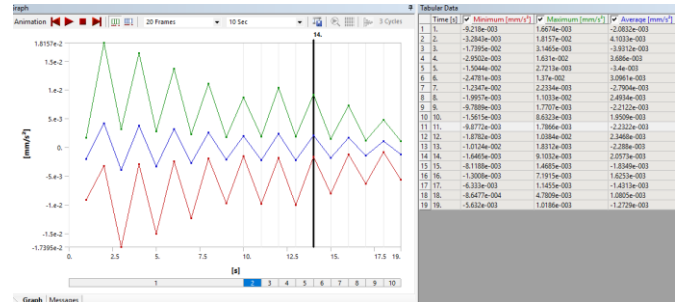


Figure 17 Graph for acceleration

### 4.3.3 Analysis of stress intensity

As described in figure (18), the stress intensity was found to be 0.000037 Mpa while in some areas where forces are applied, the stress intensity is 0.030 MPa. A large amount of stress intensity may seem counterintuitive at first. However, if we define stress intensity as per Equation 7 as follow where:

$\sigma = \text{stress intensity,}$

$F_i = \text{Force input on breast implant } A_m =$

$\text{perpendicular area of mesh on breast implant where the force is subjected upon}$

Equation 7 Equation of Stress Intensity

$$\sigma = \sum \frac{F_i}{A_m}$$

Since the mesh area value is extremely small, the calculated stress intensity should be substantial according to Equation 7. Since stress intensity is the scalar quantity, we don't need to define the directional aspect of the stress intensity.

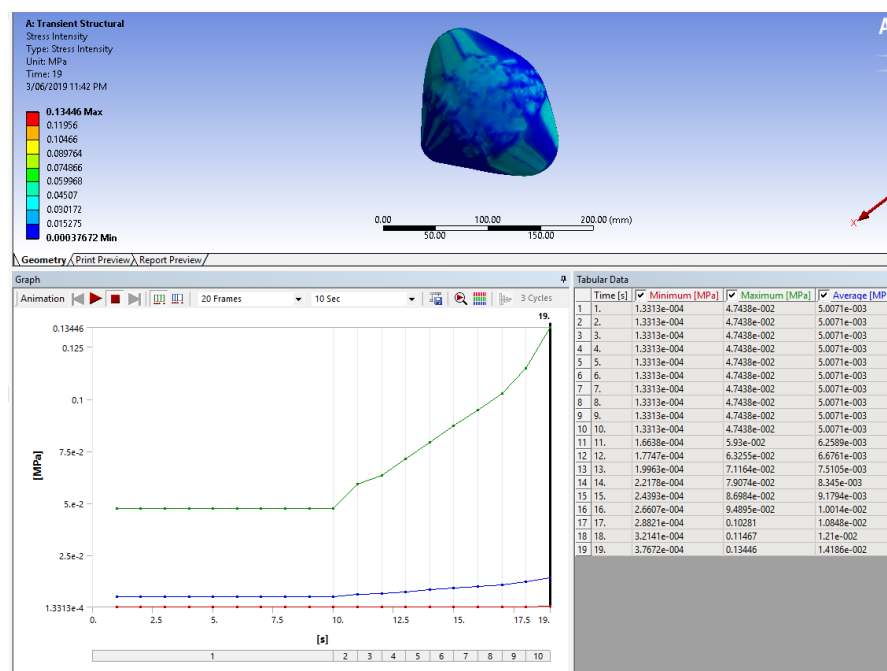


Figure 18 Stress Intensity

#### 4.3.4 Strain Energy

As for strain energy, as shown in Figure 19, it is found out that the strain energy is highest in the support area of the breast implant. The strain energy can be defined as “energy stored by the material before going deformation”. We have also found that the strain energy has increased as the input force is increased over time.

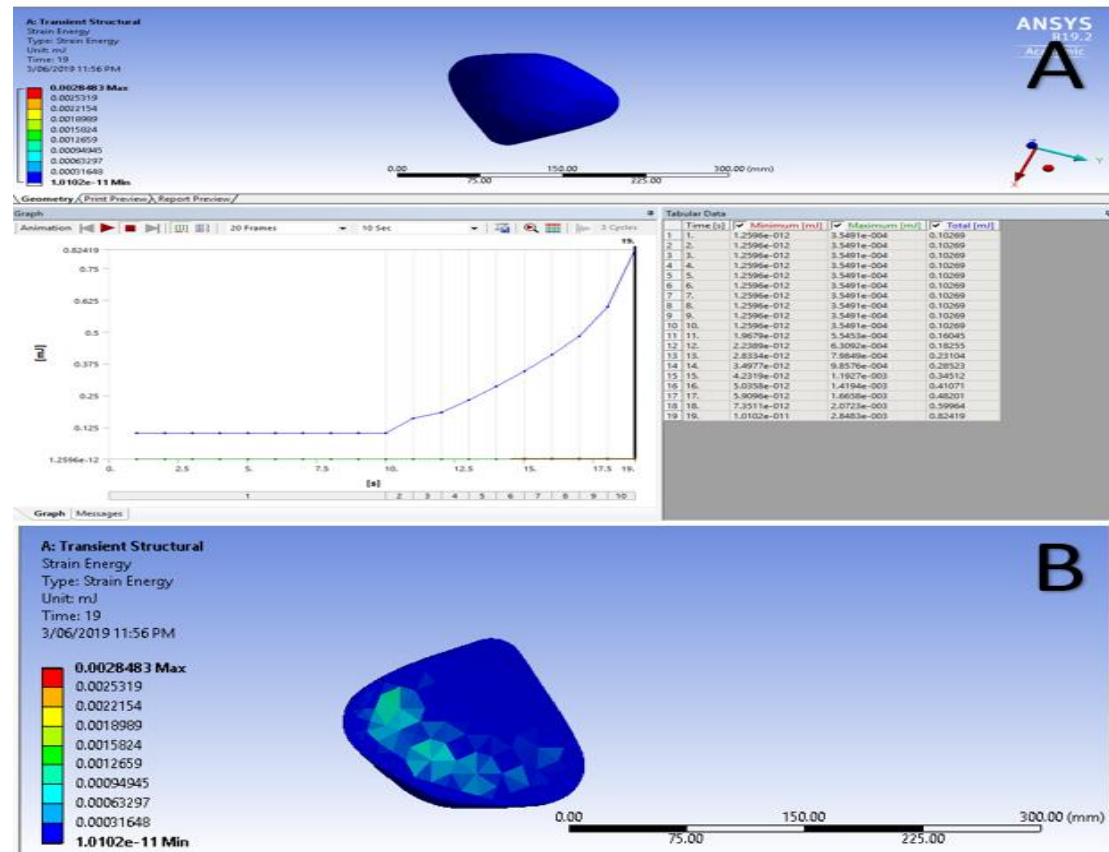


Figure 19 Strain Energy

#### 4.3.5 Maximum Shear Stress

As for maximum shear stress, as shown in Figure 20, it can be seen that the shear stress corresponds directly to the forces subject to the breast implant. According to the graph, the shear stress propagations are increasing over time along with their incremental force input, which gives the minimum final value of 0.000188MPa and maximum value of 0.007Mpa after 19 seconds.

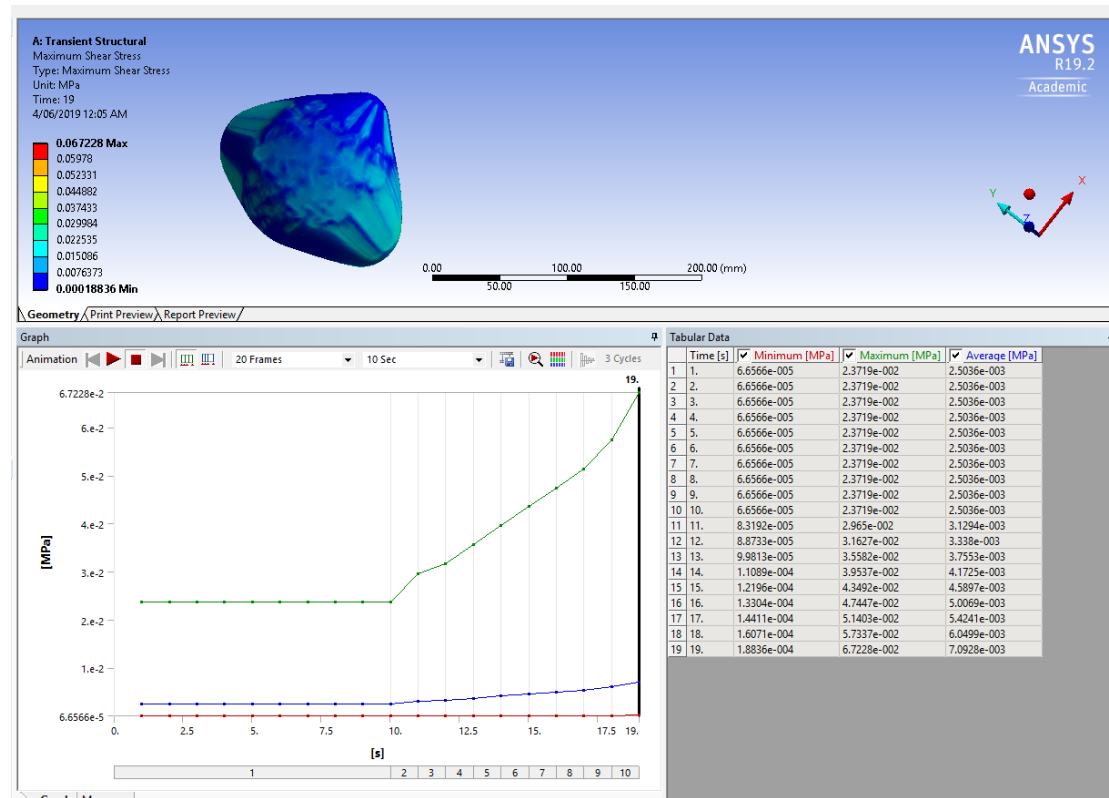


Figure 20 Maximum Shear Stress

#### 4.3.6 Normal Elastic Strain

As for the normal elastic strain result, as shown in Figure 21, it can be seen that the results fit the stress criteria. The elastic strain displacement is moving to the downward direction of 0.0001 mm from the surface of the implant. Meanwhile, the bottom part of the implant with a fixed support structure is producing the opposite directional force resulting in an upward push of 0.00031mm.

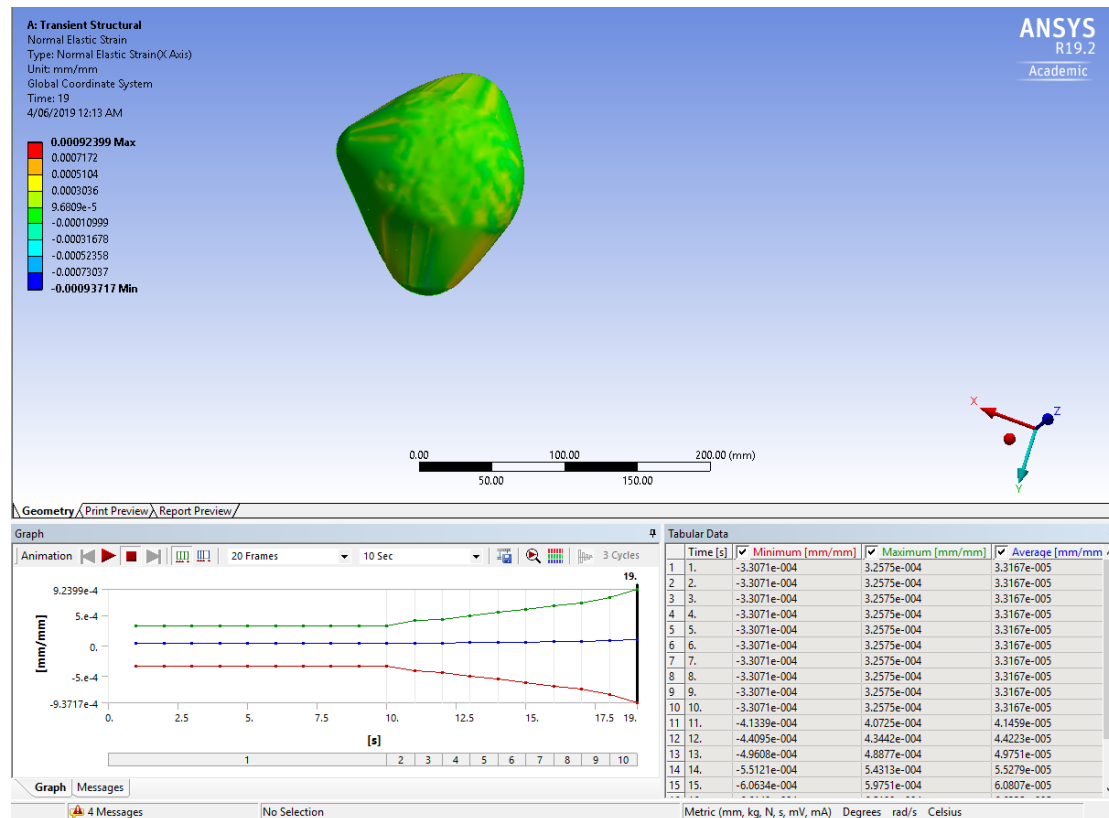


Figure 21 Normal Elastic Strain

#### 4.3.7 Interpretation of normal stress

According to Figure 22, normal stress is mostly seen at the edge of the breast structure. The red colour shows that the normal stress is acting towards the 0.04 MPa upward direction. The colour indicates that the support structure is reacting the input force through opposite force direction with higher magnitude. Again, the large number is due to the small area of the mesh size as already aforementioned in section (4.3.3 Analysis of stress intensity).

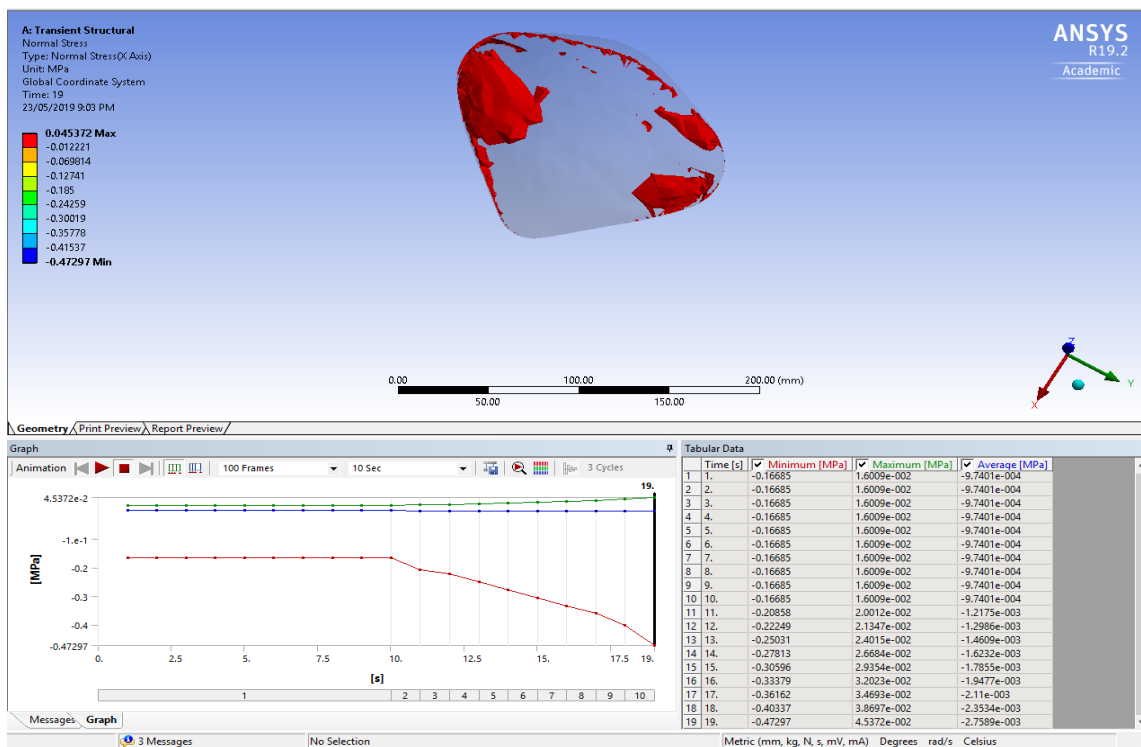


Figure 22 Normal Stress Acting on the Implant



#### 4.3.8 Interpretation of velocity propagation

As seen in (Figure 23 the velocity propagation), the nature of velocity propagation corresponds to the directional acceleration as described in section (4.3.2 Interpretation of directional velocity dissipation in breast implant). Apparently, since velocity is derivative of acceleration, the results of velocity propagation correspond according to the acceleration direction. Details velocity values are as shown in the contour graph as in Figure 23.

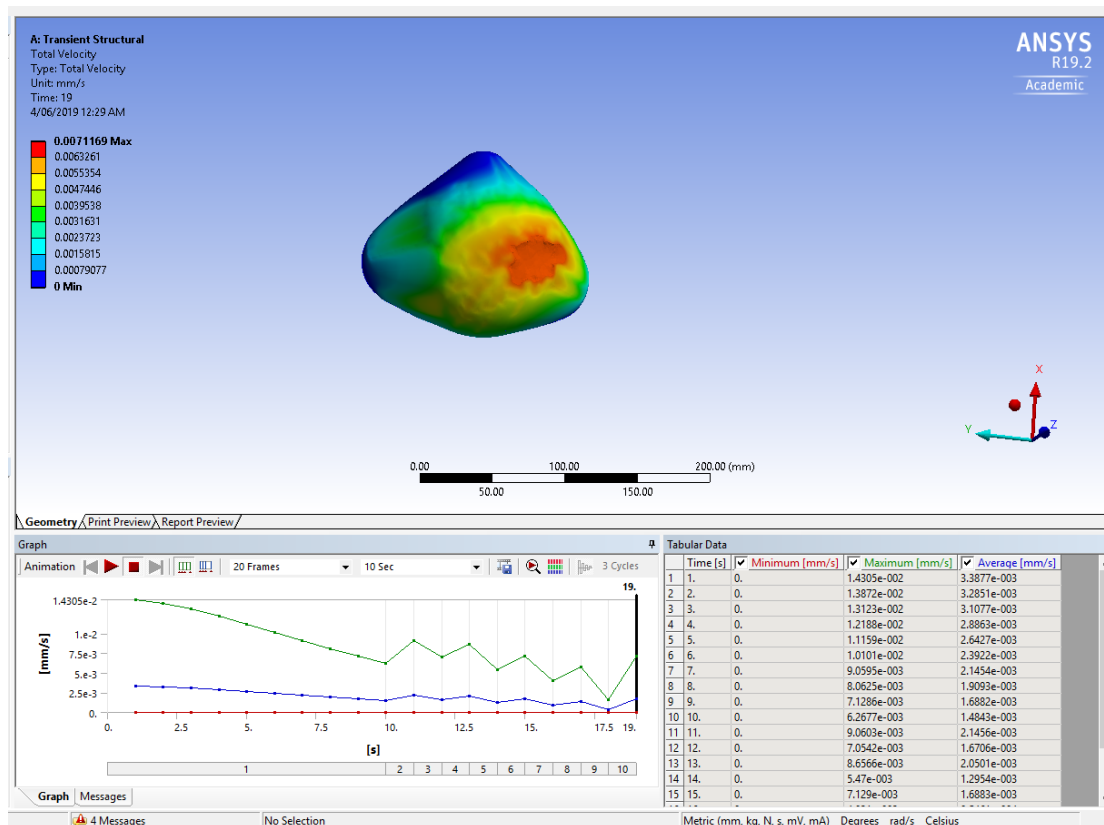


Figure 23 the velocity propagation

#### 4.3.7 Fatigue Strength Calculation using ANSYS

Fatigue strength was calculated using the random input design life parameters to produce cyclic stress-strain curve, as shown in Figure 24 below. This cyclic stress-strain curve can be further applied to get fatigued strength calculation results.

The parameters required to generate this curve are randomly selected, which includes strength coefficient=500pa, strength exponent=3, ductility coefficient=2 and cyclic hardening exponent=4. These coefficient chosen parameters were not correct and did not reflect the silicone elastomer material. However, these parameters can be re-adjusted based on the novel materials to be tested. Determination of this parameter should be consulted with the expertise of mechanics and material scientist.

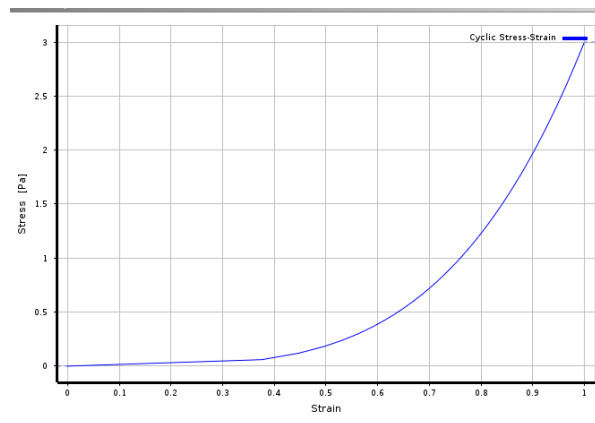


Figure 24 Cyclic Stress Curve generated using the fatigue strength coefficient

Using cyclic stress-strain parameters and other material properties data, we have calculated the design life cycle of  $10^9$  cycles along with a maximum achievable cycle of  $10^{32}$ , as shown in Figure 25. Apparently, this output may contain significant error, as constant values are not inputted with justification. The calculation made here is for demonstration purpose only since the cyclic strain

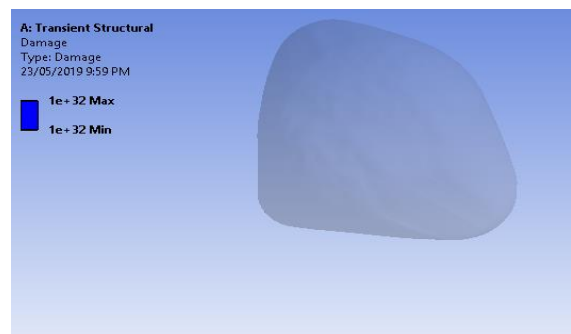


Figure 25 Duty Cycle of the breast implant under subjected load and material properties.

parameters are assumed rather than being tested. The duty cycle can be calculated once a given a set of input parameters are known.

## 4.4 Discussion

### 4.4.1 Future Opportunities

Evidently, the results at this moment generated are the results of a simplistic model rather than a realistic model. The purpose of work done here is to form the base foundation to simulate the future bio implant prototypes using the novel material. This unique material may have properties such as mechanical, thermal and optical performances which can be simulated under different physiological condition.

This project was done to create something useful with the purpose of long term scalability.

For a designer, it is crucial not only to look into what is currently available but also to seek out what is unknown and distant future of the next generation to create timeless designs. The philosophical view is supported by the famous quote of French philosopher

Michel Foucault “*There are more ideas on earth than intellectuals imagine*” (Eribon & Foucault, 1978).

Despite the promising claims as mentioned here in this report, it is also important to remember that models are only designed to approximate the natural phenomenon. It is very ludicrous to assume that models contain the soul of nature as a model is never nature itself.

There are many models which are used to approximate the product behaviour such as linear- non-linear multifactorial statistical models (Rothman, 1985), computation fluid model (Han, et al., 2012), and finite element models (Samani, et al., 2001), microbial dispersion model (Corapcioglu & Haridas, 1985) just to name a few.

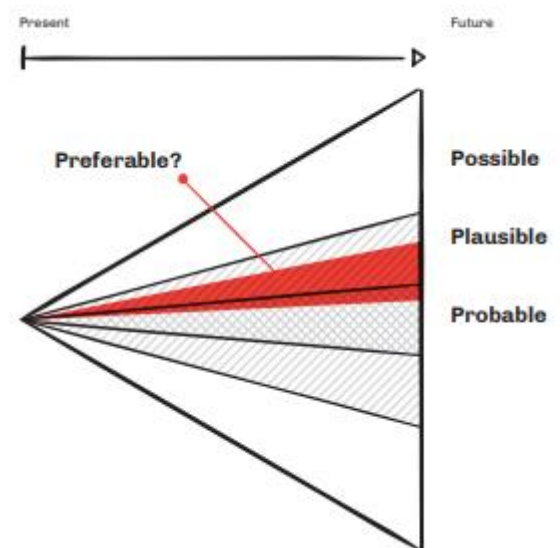


Figure 26 Curve for Speculative and Critical Design (Johannessen, n.d.)

These models may be used to approximate the conditions under different circumstances closely. However, it is crucial to note that there are many natural phenomena that we have yet to understand where the model cannot identify.

Therefore to tackle the challenges relating to those unknown phenomena, we must hold on to the first principal's validation processes no matter how intensive they can be.

As for this project, the Validation technologies to study the forces may involve: (i.e. in-vivo and in-vitro compression testing via micromanipulation & Nano-manipulation method (Thomas, et al., 2010) can be studied for further details in the reference section.

Additionally testing the viscoelastic mechanical properties of cells using micropipette aspiration, cyto-indentation, magnetic bead rheometry and optical traps method (Darling, et al., 2007) using the modern instruments such as AFM and SEM are also required for further validation of the microbial adhesion forces.

As society advances and moves towards the dawn of a new civilisation, many technical advances will be seen. The notable examples of technological landscape include the age of industrial 4.0, development of society 5.0, completion of human genomic sequencing, CRISPR, digitalisation of material and chemical analytical instruments, supercomputing, cloud data storage and advancement of artificial intelligence.

Along with the singularity point of transdisciplinary technologies, modelling, the human physiology is in plausible status under the designer's point of view, as shown in Figure 26.

#### 4.4.2 Current Challenges

Despite the positive notions on the modelling of material properties such as mechanical, thermal and optical properties, many challenges are still required to be addressed. These include:

##### **Type of study to be taken with ANSYS**

The current research being undertaken is transient force analysis. However, based on the prototype requirement, a different kind of ANSYS modelling suite may be used, as shown in Figure 42 at (Appendix H: Different ANSYS Modelling Suite).

##### **Challenges Relating to Mesh**

Challenges relating to mesh involve changing the geometry of the mesh based on human anatomy and MRI- ANSYS combo modelling. Additionally, it is necessary to understand the tradeoffs between mesh sizing & computation efficiency and validating the mesh convergence to approximate the physiological phenomenon.

##### **Challenges relating to the numerical approximation**

The current method used is the Newton Raphson methods. Other numerical optimisation methods may be used for this stress analysis for optimum performance. Different numerical optimisation methods may be performed to compare the convergence and time taken for the results. From this challenge, this project may open new project relating to numerical convergence.

**Challenges relating to the material data**

In these models, factors corresponding cyclic stress-strain curve were not described for the silicone. These factors need to be validated and tested. Apparently, there are basic material properties such as Poisson ratio, young modulus, tensile strength, hardness, which are commonly used for analysis. However, it is essential to understand the material properties based on the design objectives such as shape memory properties, creep properties, thermal properties, plasticity properties and fracture criterion. These properties will allow us to study the damage and life-cycle of the prototypes constructed by that new material. Therefore, this project may open the new field to research on a prototype using the above materials properties which we may have never thought before.

**Challenges relating to the Input force**

Input force of microbial cells and breast-implant are needed to be tested in real time under different load conditions using various methods and tools.

This process will allow us to understand proper force distribution on the breast implant surface. Finally, Osmotic pressure forces of bodily fluid may also be required to study in detail, which will allow us to create more realistic force input.

## 5.0 Conclusions

In conclusion, the simplistic and theoretical transient stress model of breast implant by applying a combination of Solid-Work, SCAD and ANSYS software using the traditional silicone material properties data has been demonstrated through graphical and numerical data. The demonstration is carried out through showing the results of deformation, directional acceleration, stress intensity propagation, maximum shear stress, normal elastic strain and velocity propagation of the breast implant. These results are shown as they play critical roles in determining the vascular contracture. Therefore, by understanding this shockwave propagation, we may be able to predict vascular contracture inside the human body by looking into the initial position of bacteria and the nature of their growth. In this way, we may be able to do the preventative surgery or treatment before the actual vascular contracture begins.

From the progress of this modelling to digital twin integrated with real-time MRI image of the breast, both surgeon and user can efficiently predict and evaluate for preventative treatment before capsular contracture and rupture begins. Moreover, CFD and transient motions can be demonstrated to patients to pursue the better satisfaction of the client.

Apparently, several challenges to be overcome to achieve this level of innovation may be aplenty. However, as engineers and scientist, it is our responsibility to correctly predict and evaluate the unknown threats so that family and children can safely and happily go back to their home.



## 6.0 Bibliography

1. A Berkshire Hathaway Company, 2008.  
*<https://www.businesswire.com/news/home/20080924005090/en/Largest->*
2. *ANSYS-International-Conference-Date-Underscores-Increasing*. [Online]  
Available at:  
*<https://www.businesswire.com/news/home/20080924005090/en/Largest-ANSYS-International-Conference-Date-Underscores-Increasing>*  
[Accessed 2019].
3. Abaqus 6.10, 2018. *Overview of Continuum Shell Modeling*. [Online]  
Available at:  
*<https://www.sharcnet.ca/Software/Abaqus610/Documentation/docs/v6.10/books/usi/default.htm?startat=pt04ch24s01.html>*
4. Anon., 1998. Accurate finite-element multi-grid FEM-MG description for angular momentum and spin dependences of Kohn–Sham density functionals for axially restricted calculations on first-row atoms and dimers. *Chemical Physics Letters*, Volume 295, pp. 439-446.
5. ANSYS Advantage Staff, 2012. Model+Make. *ANSYS ADVANTAGE*, VI(1).
6. ANSYS Inc, 2015. *ANSYS HFSS*. S.l.: ANSYS.
7. ANSYS, 2018. *Build Your Own Flight Simulator on Prepar3D to Streamline Cockpit Design*. [Online]  
Available at: *<https://www.ansys.com/en/blog/flight-simulator-on-prepar3d-built-with-ansys-scade>*
8. Avinash, 2018. *What is the time step in FEA?*. [Online]  
Available at: *<https://www.quora.com/What-is-time-step-in-FEA>*
9. Baxter, R. A., 2003. Intracapsular Allogenic Dermal Grafts for Breast Implant-Related Problems. P. *Plastic and Reconstructive Surgery*, Volume 6, p. 112.
10. Behr, M. & Tezduyar, T., 1992. Finite element solution strategies for large scale flow simulations. *Computer Methods in Applied Mechanics and Engineering*, 112(2), pp. 3-24.
11. Boschert, S. & Rosen, R., 2016. *Digital Twin-The Simulation Aspect*. S.l.: Mechantronic Futures.
12. Brook, M. A., 2006. Platinum in silicone breast implants. Volume 27, pp. 3274-3286.
13. Bruck, H., McNeill, S., Sutton, M. & Peters, W., 1989. Digital Image Correlation Using Newton-Raphson Method of Partial Differential Correction. *Experimental Mechanics*, 29(3), pp. 261-267.

14. Bucki, M., Lobos, C., Payan, Y. & Hitchfeld, N., 2011. *Jacobian-based repair method for finite element meshes pair after registration*. S .l.: Engineering with Computers.
15. Castel, N. et al., 2015. Polyurethane-Coated Breast Implants Revisited: A 30-Year Follow-Up. *Archives of Plastic Surgery*, pp. 186-193.
16. Cheng, N.-x. Et al., 2002. Complications of Breast Augmentation with Injected Hydrophilic Polyacrylamide Gel. Volume 26, pp. 375-382.
17. Chen, H. & Wang, X., 2002. *Cooperative coevolutionary algorithm for unit commitment*. S .l., Transaction on Power System, pp. 128-133.
18. Cherup et al., 1989. *Measurement of capsular contracture: the conventional breast implant and the Pittsburgh implant*. S .l.: Plastic and Reconstructive Surgery.
19. Cianco, D., Carol, I. & Cuomo, M., 2007. Crack opening conditions at 'corner nodes' in FE analysis with cracking along mesh line. *Engineering Fracture Mechanics*, 74(13), pp. 1963-1982.
20. Corapcioglu, Y. & Haridas, A., 1985. Microbial transport in soils and groundwater: A numerical model. *Advances in water resources*, 8(4), pp. 188-200.
21. Cryer, C. W. & Tavernini, L., 1972. The Numerical Solution of Volterra Functional Differential Equation by Euler's Method. *Siam Journal on Numerical Analysis*, 9(1), pp. 105-129.
22. Darling, E., Zauscher, S., Block, J. & Guilak, F., 2007. A Thin-Layer Model for Viscoelastic, Stress-Relaxation Testing of Cells Using Atomic Force Microscopy: Do Cell Properties Reflect Metastatic Potential ?. Volume 92, pp. 1784-1791.
23. Daniel, H., 2017. *Finite Element Analyses - Not All Beautiful Color Plots are Precise or Accurate*. [Online]  
Available at: <https://www.nasa.gov/offices/nesc/articles/finite-element-analyses>  
[Accessed, 2019].
24. Dufrene, Y., 2015. Understanding forces in biofilms. *Nanomedicine*, 8(10), pp. 1219-1221.
25. Dunn, T. & J.K., T., 2000. Breast and Chest Size Satisfaction: Relation to Overall Body Image and Self-Esteem. *Eating Disorders: The Journal of Treatment & Prevention*, 8(3), pp. 241-246.
26. E, C., Morris, M. & Irazoqui, P., 2013. Implantable RF Medical Device: The Benefits of high-speed Communication and Much Greater Communication Distance in Biomedical Applications. *IEEE Microwave Magazine*, 14(4), pp. 64-73.
27. Element, 2018. *Finite Element Analysis(FEA) Services*. [Online]  
Available at: <https://www.element.com/materials-testing-services/finite-element-analysis>

28. Eribon, D. & Foucault, M., 1978. *Les Reportages d'Idees Corriere Della Sera*, Milan: s.n.
29. Farhad Zadeh, Z. et al., 2018. Growth Rate and Biofilm Formation Ability of Clinical and Laboratory-Evolved Colistin-Resistant Strains of *Acinetobacter baumannii*. *Front Microbiol*, 9(153), p. 153.
30. Foy, W., 1976. Position-Location Solutions by Taylor-Series Estimation. IEEE. *IEEE Transactions on Aerospace and Electronic System*, pp. 187-194.
31. Garbey, M. et al., 2014. *Computational Surgery and Dual Training*. 1st ed. NY: Springer.
32. Gardener, J., Craven, M., Dow, C. & Hines, E. L., 1998. The prediction of bacteria type and culture growth phase by an electronic nose with a multi-layer perceptron network. *Measurement Science and Technology*, 9(1), pp. 120-127.
33. Global Market Insight, 2019. *Global Market Insight-Industry Trend: Breast Implant Market*. [Online]  
Available at: <https://www.gminsights.com/industry-analysis/breast-implants-market>
34. Goenezen, S. et al., 2012. Linear and Nonlinear Elastic Modulus Imaging: An Application to Breast Cancer Diagnosis. *IEEE Transactions on Medical Imaging*, 31(8), pp. 1628-1637.
35. Goodman, J. & Walsh, Childers, K., 2004. Sculpting the Female Breast: How College Women Negotiate the Media's Ideal Breast Image. *Journalism & Mass Communication Quarterly*, 81(3), pp. 657-674.
36. Handel, N., 2006. Long-Term Safety and Efficacy of Polyurethane Foam-Covered Breast Implants. *Aesthetic surgery journal*, Volume 26, pp. 265-274.
37. Han, L. et al., 2012. Development of patient-specific biomechanical models for predicting large breast deformation. *Physics in Medicine and Biology*, Volume 52, pp. 455-472.
38. Harrison, K., 2003. Television Viewers' Ideal Body Proportions: The Case of the Curvaceously Thin Woman. *Sex Roles*, March.48(5).
39. Haupt, S. E., 2005. A demonstration of coupled receptor/dispersion modelling with a genetic algorithm. *Atmospheric Environment*, 39(37), pp. 7181-7189.
40. Hillard, C., Fowler, J. D., Barta, R. & Cunningham, B., 2017. Silicone breast implant rupture: a review. *Gland Surg.*, 6(2), pp. 163-168.
41. H. N., W. R. & G. M., 2013. Breast implant rupture: causes, incidence, clinical impact, and management. *Plast Reconstr Surg*, 132(5), pp. 1128-1137.
42. HU, H. et al., 2015. Chronic Biofilm Infection in Breast Implants is Associated with an Increased T cell Lymphocytic Infiltrate: Implication for Breast Implant-Associated Lymphoma. *Plastic and Reconstructive Surgery*, 135(2), pp. 319-329.

43. Jackson, L. & Ervin, K., 1992. Height Stereotypes of Women and Men: The Liabilities of Shortness for Both Sexes. *The Journal of Social Psychology*, Volume 132, pp. 433-445.
44. Jacombs, A. et al., 2012. Prevention of Biofilm-induced Capsular Contracture With Antibiotic Impregnated Mesh in a Pocine Model. *Aesthetic Surgery*, 32(7), pp. 886-891.
45. Johannessen, L. K., n.d. *The young Designer's Guide to Speculative and Critical Design*, s.l.: Department of Design: Norwegian University of Science and Technology.
46. Kintel, M., 2019. *OpenSCAD: The Programmers Solid 3D CAD Modeller*. [Online]  
Available at: <http://www.openscad.org/about.html>  
[Accessed 10 04 2019].
47. Knupp, p., 1999. *Matrix norms & the condition number, a general framework to improve mesh quality via node movement*. S.l., s.n., pp. 13-22.
48. Lee, H. H., 2018. *Finite Element Simulations with ANSYS Workbench 18*. 1st ed. Taiwan: SDC.
49. Lee, J., Bagheri, B. & Kao, H. A., 2015. A Cyber-Physical Systems architecture for Industry 4.0-based manufacturing systems. *Elsevier*, Volume 3, pp. 18-23.
50. Liu, C. Y. & Hwang, C. J., 2001. New Strategy for Unstructured Mesh Generation. *AIAA Journal*, 39(6), pp. 1078-1085.
51. Macdonald, P. et al., 1995. Failure of  $^{29}\text{Si}$  NMR To Detect Increased Blood Silicon Levels in Silicone Gel Breast Implant Recipients. Volume 67, pp. 3799-3801.
52. Neuman, S., 1984. Adaptive Eulerian-Lagrangian Finite Element Method For Advection Dispersion. *Journal for Numerical Methods in Engineering*, Volume 20, pp. 321-337.
53. Nielsen, R. V., Rajagopal, V. & Nash, M., 2009. Modelling breast biomechanics for multimodal image analysis successes and challenges. *Systems Biology and Medicine*, 2(3), pp. 293-304.
54. Ozen, M., 2014. *Meshing Workshop*. s.l., Ozen Engineering.
55. Parthasarathy, J., Starly, B. & Raman, S., 2011. A design for the additive manufacture of functionally graded porous structures with tailored mechanical properties for biomedical applications. *Journal of Manufacturing Process*, 13(2), pp. 160-170.
56. PERUSIC, 2017. *Finite Element Analysis*. [Online]  
Available at: <http://www.pengineering.com.au/services/finite-element-analysis>
57. Pietrzak, A., 2019. *Pratt & Whitney Standardizes on ANSYS Engineering Simulation*. [Online]

Available at: <https://www.ansys.com/about-ansys/news-center/05-02-17-pratt-whitney-standardizes>

58. Prasad, K. et al., 2019. Cosmetic reconstruction in breast cancer patients: Opportunities for nanocomposite materials. *Acta Biomaterialia*, Volume 86, pp. 41-65.
59. Quaini, V., Mantero, S. & Villa, T., 2005. Mechanical properties of breast periprosthetic capsules and the correlation to capsule contracture. *Journal of Applied Biomaterials & Biomechanics*, Volume 3, pp. 184-191.
60. Riesenber, D. et al., 1991. High Cell Density Cultivation of Escherichia Coli at controlled specific growth rate. *Journal of Biotechnology*, Volume 20, pp. 17-18.
61. Rothman, D., 1985. Nonlinear Inversion, statistical mechanics, and residual statics estimation. *Geophysics*.
62. Samani, A., Bishop, J., Yaffe, M. J. & Plewes, D. B., 2001. *Biomechanical 3-D Finite Element Modeling of the Human Breast Using MRI data*. S.l.: IEEE.
63. Samani, A., Bishop, J., Yaffe, M. & Plewes, D., 2001. Biomechanical 3-D Finite Element Modeling of the Human Breast Using MRI Data. *IEEE Transactions on Medical Imaging*, 20(4), pp. 271-279.
64. Sargent, R. G., 2004. *VALIDATION AND VERIFICATION OF SIMULATION MODELS*. S.l., IEEE.
65. Schlesinger, 1979. Terminology for model credibility. *Simulation*, 32(3), pp. 103-104.
66. Schroeder, G. et al., 2016. *Visualising the Digital Twin Using Web Services and Augmented Reality*. S.l., IEEE.
67. Schutte, J. et al., 2004. Parallel global optimisation with the particle swarm algorithm. *International Journal for Numerical Methods in Engineering*, 61(3), pp. 2296-2315.
68. Song, D. H. & Ooi, A. S., 2016. Reducing infection risk in implant-based breast reconstruction surgery challenges and solutions. *Breast Cancer: Targets and Therapy*, Volume 8, pp. 161-172.
69. Song, D. H. & Ooi, A. S., 2016. Reducing Infection Risk in Implant-based breast reconstruction surgery challenges and solutions. *Breast Cancer: Targets and Therapy*, 8(doi:10.2147/bcct.s97764), pp. 161-172.
70. S, S. et al., 2019. BThe role of bacterial biofilm and mechanical forces in modulating dental implant failures. *Journal of the Mechanical Behavior of Biomedical Materials*, , pp. 118-127.
71. Stohi, A. et al., 2005. *Technical note: The Lagrangian particle dispersion model FLEXPART version 6.2*. S.l.: Atmospheric Chemistry and Physics.
72. Tamboto, H., Vickery, K. & Deva, A. K., 2010. Subclinical (Biofilm) Infection Causes Capsular Contracture in a Porcine Model following Augmentation Mammoplasty. *Plastic and Reconstructive Surgery*, 126(3), pp. 835-842.

73. Thomas, C., Stenson, J. & Zhang, Z., 2010. *Measuring the Mechanical Properties of Single Microbial Cells*. S .l.: Advances in Biochemical Engineering/Biotechnology.
74. Tristan, 2018. *Orthogonality Angle*. [Online]  
Available at: <https://www.cfd-online.com/Forums/cfx/26747-orthogonality-angle.html>
75. Weems, A. et al., 2017. Shape memory polyurethanes with oxidation-induced degradation: In vivo correlations for endovascular material applications. *Biomaterialia*, Volume 59, pp. 33-44.
76. Wilson, K. A., 1999. *FINITE ELEMENT ANALYSIS OF BREAST IMPLANTS*. S .l.: Virginia Polytechnic Institute and State University.

## 7.0 Appendices

### Appendix A: Figures Related to Meshing Process

Details of "Mesh"	
<b>Display</b>	
Display Style	Use Geometry Setting
<b>Defaults</b>	
Physics Preference	Mechanical
Solver Preference	Mechanical APDL
Element Order	Program Controlled
<input type="checkbox"/> Element Size	Default
<b>Sizing</b>	
Use Adaptive Sizing	Yes
Resolution	Default (2)
Mesh Defeaturing	Yes
<input type="checkbox"/> Defeature Size	Default
Transition	Fast
Span Angle Center	Coarse
Initial Size Seed	Assembly
Bounding Box Diagonal	215.25 mm
Average Surface Area	14.214 mm <sup>2</sup>
Minimum Edge Length	5.6782e-004 mm
<b>Quality</b>	
Check Mesh Quality	Yes, Errors
Error Limits	Standard Mechanical
<input type="checkbox"/> Target Quality	Default (0.050000)
Smoothing	Medium
Mesh Metric	None
<b>Inflation</b>	
Use Automatic Inflation	None
Inflation Option	Smooth Transition
<input type="checkbox"/> Transition Ratio	0.272
<input type="checkbox"/> Maximum Layers	5
<input type="checkbox"/> Growth Rate	1.2
Inflation Algorithm	Pre
View Advanced Options	No
<b>Advanced</b>	
Number of CPUs for Parallel Part Meshing	Program Controlled
Straight Sided Elements	No
Number of Retries	Default (4)
Rigid Body Behavior	Dimensionally Reduced
Triangle Surface Mesher	Program Controlled
Topology Checking	Yes
Pinch Tolerance	Please Define
Generate Pinch on Refresh	No
<b>Statistics</b>	
<input type="checkbox"/> Nodes	50904
<input type="checkbox"/> Elements	29185

Figure 27: Mesh Properties Table Data

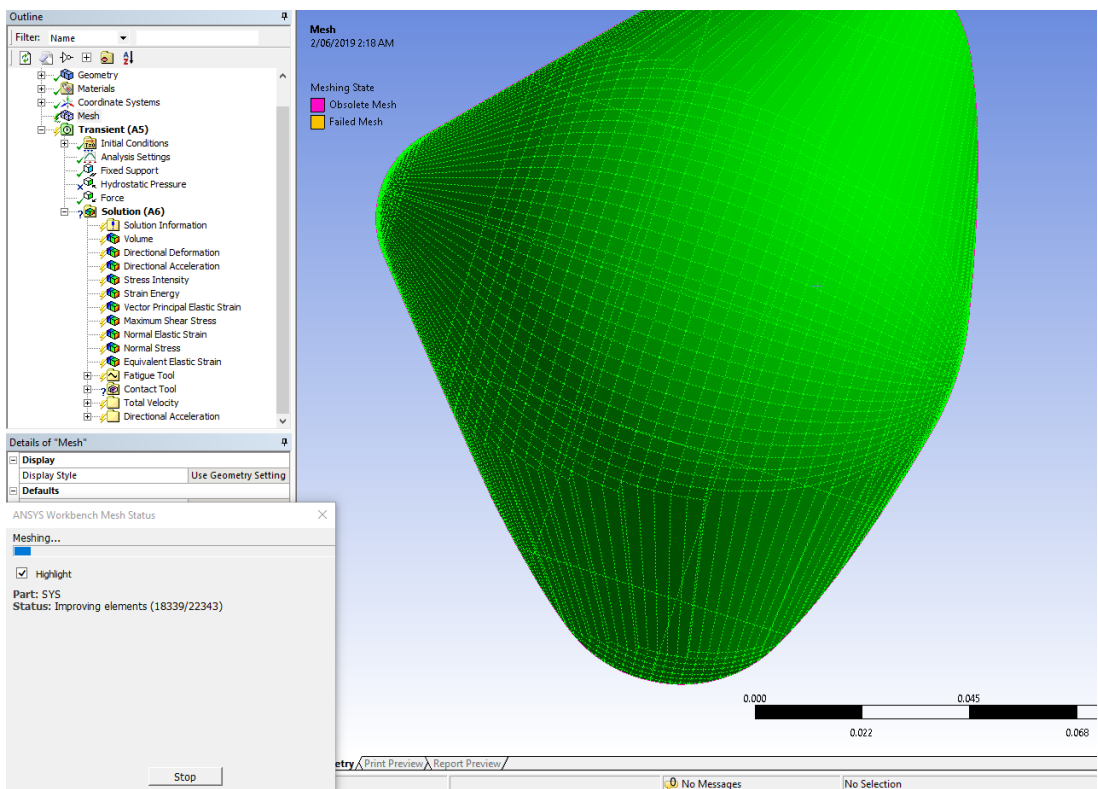


Figure 28 Mesh Solving Status

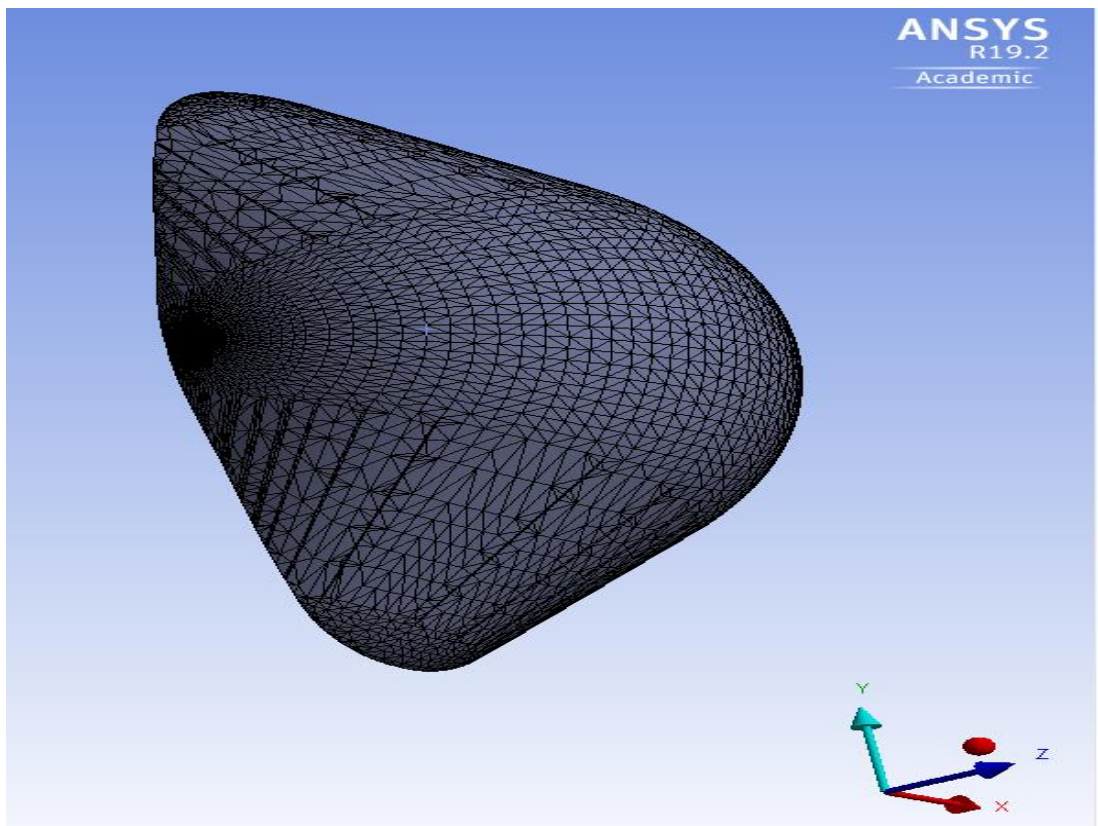


Figure 29 Meshed Breast



Table 2 Value of Skewness and Cell Quality (Ozen, 2014)

Value of Skewness	Cell Quality
1	Unacceptable
0.9-<1	Bad
0.75-0.9	Poor
0.5-0.75	Fair
0.25-0.5	Good
>0-0.25	Excellent
0	Equilateral

Skewness mesh metrics spectrum



Orthogonal Quality mesh metrics spectrum



Figure 30 Relationship between Colours of the mesh and mesh quality (Ozen, 2014)

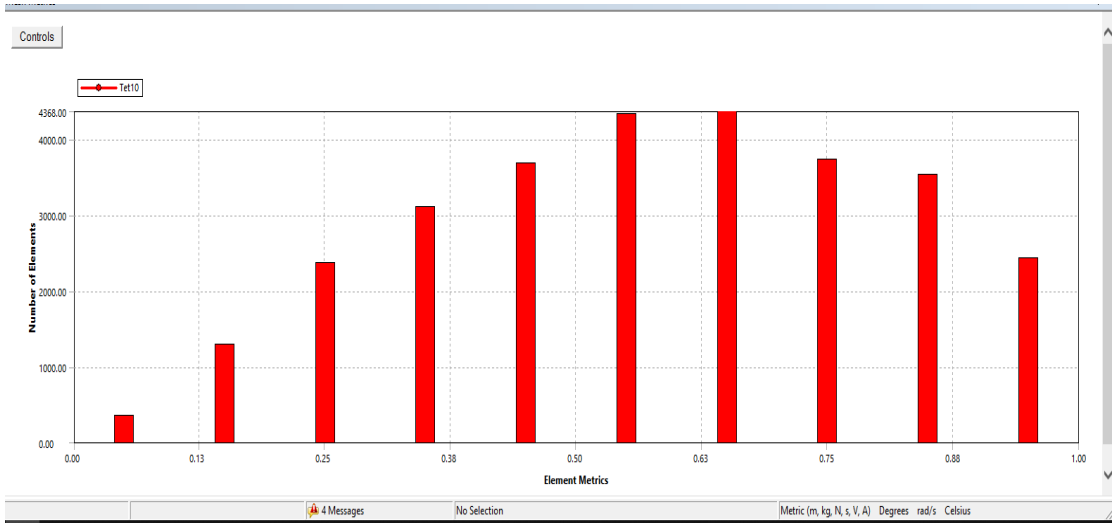


Figure 31 Mesh Skewness Size Distribution of our designed breast implant

## Appendix B: SCAD file source code to Design Breast Implant

```
//Two methods to measure for breast prosthetic either width of desired breast size (substitute in b directly) or Length over top
of breast l=b*(3/4)

// Using width of breast size or length over top of breast?
measure_choice = "width"; // [width,length]

// What is the value in mm?
value = 150;

// Flat or rounded back?
flat_or_rounded = "flat"; // [flat,rounded]

//ignore these
b = (measure_choice == "width" ? value : value*4/3);
w = b*2/3; //hiddens sphere
$fn = 100/1;

module breast(){
  difference(){
    hull(){
      sphere(w/1.75); //Sphere main
      translate([w/5,w/2,-w/8]) sphere(w/3); //sphere left
      translate([w/5,-w/2,-w/8]) sphere(w/3); //sphere right
      translate([0,0,w/2]) sphere(w/5); //sphere top
    }
    if (flat_or_rounded == "flat") {
      translate([w,0,0]) cube([w*2,w*2,w*2],center=true); //cleaving back with flat back
    }
    else {
      translate([w*5,0,0]) sphere(w*5); //cleaving back with big sphere for round back
    }
  }
}

rotate([0,90,0])breast(); //print flat
```

Figure 32 Scad File Source CODE

## Appendix C: Silicone Property Data

Table 3 Wacker Silicone Material Properties and Standards

Appearance	Transparent
Density	1.-10-1.14
Viscosity	600,000-1,600,000
Hardness	30-45
Tensile Strength	45-60
Elongation Strength	18-30
Tear Strength	23
Rebound Resilience	$5 \cdot 10^{15}$
Compression Set	10-30
Dielectric Strength	23
Volume Resistivity	$5 \cdot 10^{15}$
Dielectric Constant	3.1
Dissipation Factor	$30 \cdot 10^{-4}$
Limiting Oxygen	27

## Appendix D: Material Property Options to be selected for Future Use

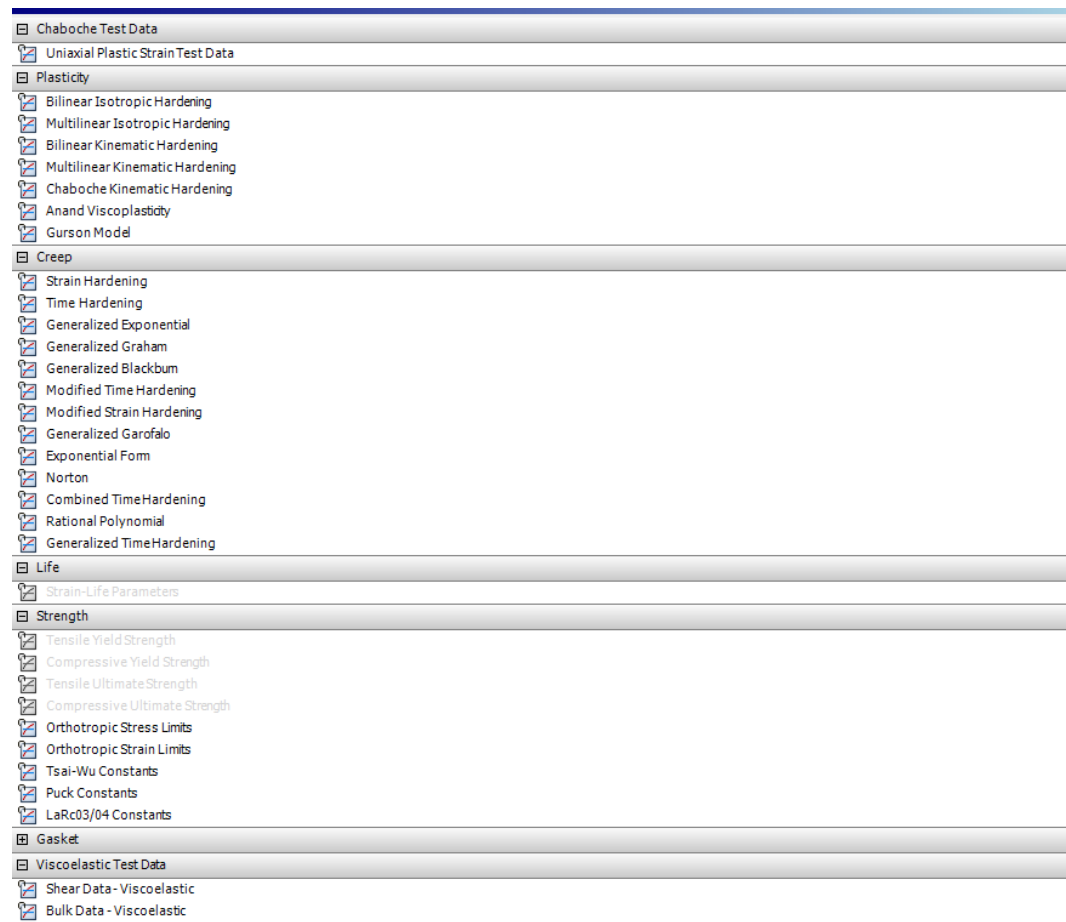


Figure 34 Material Data input option screenshot-1

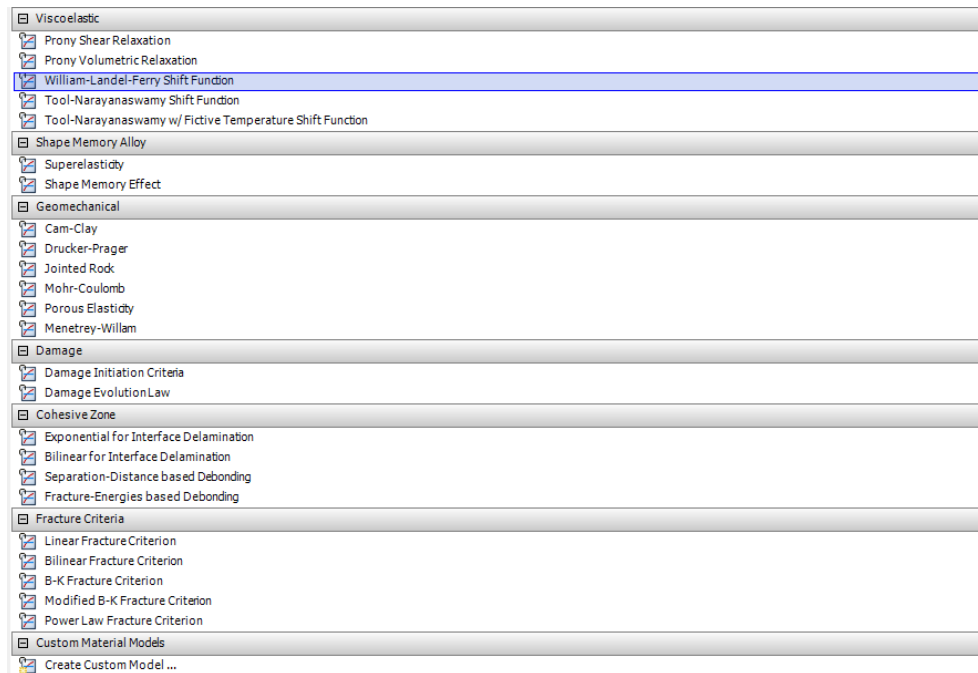


Figure 33 Material data input screenshot 2

Figure 35 Engineering Data and ANSYS product Suite

Appendix E: Theoretical Silicone Non-linear Stress-Strain Curve

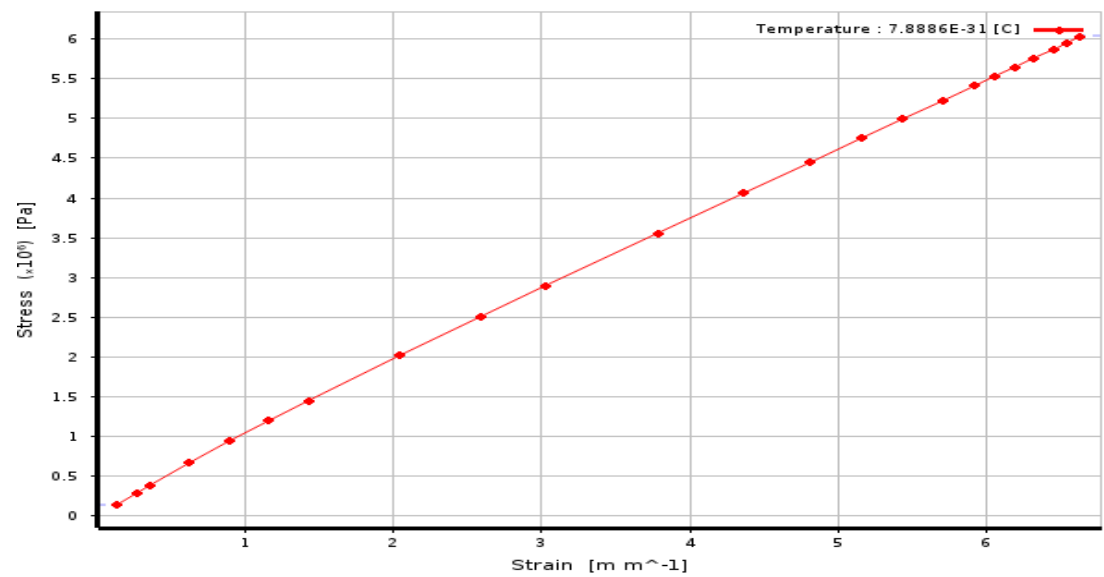
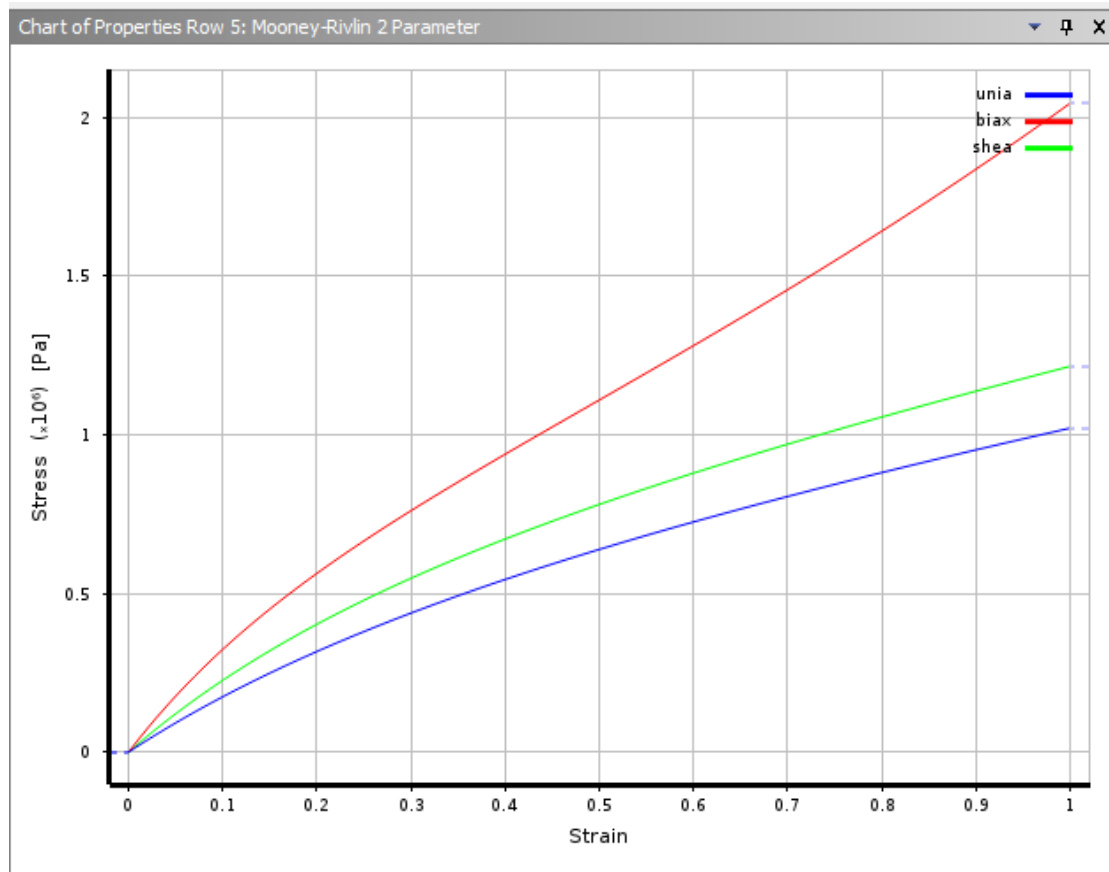


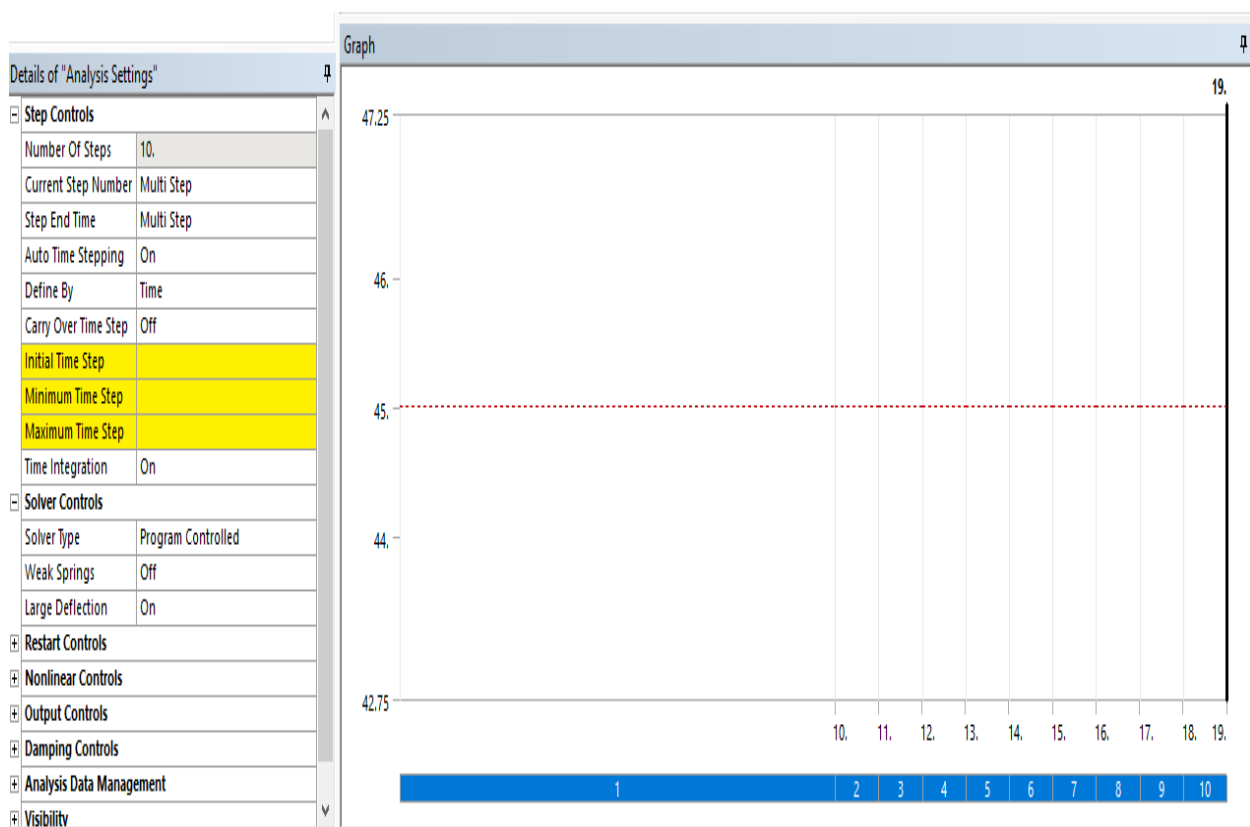
Figure 36 Neo Hooke and Relationship of Elastomer

**Table 4 Mooney-Reivling stress-strain response of Silicone material to check the fatigue strength**



**Figure 37 Uniaxial biaxial and shear curve of Silicone Material**

## Appendix F: Step Sizing, Numerical Method Control, Damping Control, Visibility Management Options



Appendix: E Solutions for Initial Iteration of the model first test

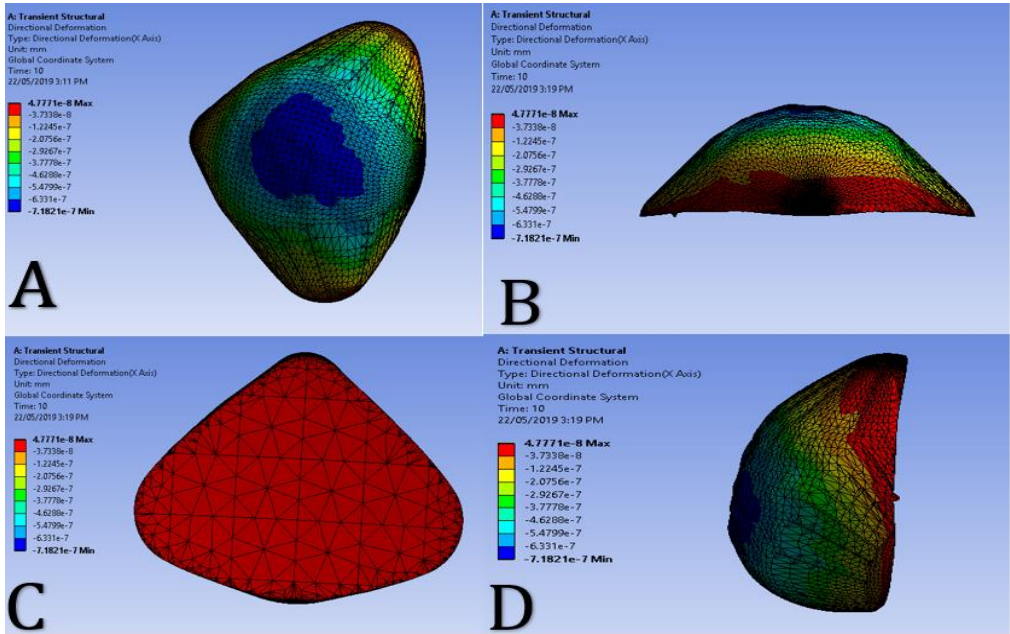


Figure 39 Directional Deformation for 10 steps Transient force

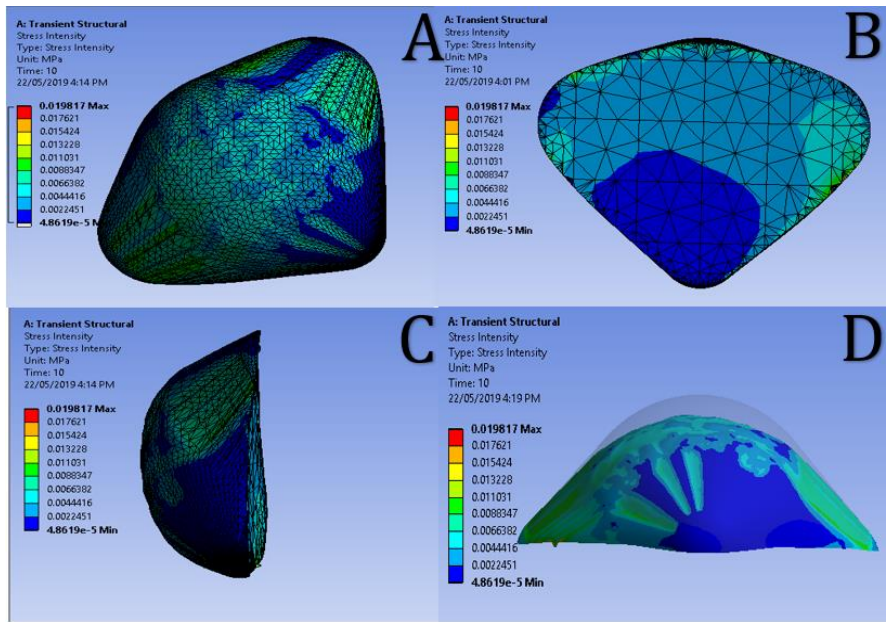


Figure 40 Stress Intensity of the breast



## Appendix G: Breast Size Chart Samples

ES 80 Low Profile 85% filled				ES 801 Medium Profile 100% filled				ES 81 High Profile 85% filled				ES 811 Extra High Profile 100% filled			
	Dia (cm)	Proj (cm)	Vol (cc)		Dia (cm)	Proj (cm)	Vol (cc)		Dia (cm)	Proj (cm)	Vol (cc)		Dia (cm)	Proj (cm)	Vol (cc)
80100	9.6	2.0	100	801100	8.5	2.8	100	81100	7.9	2.9	100	811100	7.3	3.4	100
80120	9.7	2.4	120	801120	9.0	2.9	120	81120	8.9	2.8	120	811120	8.0	3.5	120
80140	10.2	2.5	140	801140	9.3	3.2	140	81140	8.8	3.2	140	811140	8.5	3.8	140
80160	10.4	2.8	160	801160	10.0	3.1	160	81160	9.3	3.3	160	811160	8.8	3.9	160
80180	10.9	2.9	180	801180	10.6	3.2	180	81180	9.5	3.6	180	811180	9.1	4.3	180
80200	11.6	2.8	200	801200	11.1	3.3	200	81200	9.9	3.7	200	811200	9.4	4.3	200
80220	11.8	3.0	220	801220	11.5	3.2	220	81220	10.3	3.7	220	811220	9.7	4.4	220
80240	12.0	3.1	240	801240	11.7	3.5	240	81240	10.5	3.9	240	811240	10.2	4.4	240
80260	12.2	3.3	260	801260	11.9	3.6	260	81260	10.7	4.1	260	811260	10.4	4.5	260
80280	12.5	3.3	280	801280	12.3	3.7	280	81280	10.9	4.3	280	811280	10.6	4.7	280
80300	12.9	3.4	300	801300	12.4	3.9	300	81300	11.1	4.4	300	811300	10.8	4.9	300
80325	13.2	3.5	325	801325	12.7	4.0	325	81325	11.4	4.5	325	811325	11.0	5.1	325
80350	13.5	3.6	350	801350	13.0	4.0	350	81350	11.7	4.7	350	811350	11.3	5.1	350
80375	13.8	3.7	375	801375	13.3	4.2	375	81375	11.7	4.9	375	811375	11.6	5.2	375
80400	14.2	3.7	400	801400	13.7	4.2	400	81400	12.2	4.9	400	811400	11.8	5.5	400
80450	14.7	3.8	450	801450	14.1	4.4	450	81450	12.5	5.3	450	811450	12.1	5.7	450
80500	15.3	4.0	500	801500	14.5	4.6	500	81500	12.6	5.8	500	811500	12.3	6.1	500
				801550	15.0	4.8	550					811550	12.5	6.4	550
				801600	15.8	4.5	600					811600	13.1	6.4	600
				801650	15.8	4.9	650					811650	13.6	6.4	650
				801700	15.8	5.4	700					811700	13.4	7.1	700
				801750	15.9	5.8	750					811750	13.5	7.4	750
				801800	15.8	6.0	800					811800	13.6	7.7	800

Figure 41 Breast Size Chart Examples

## Appendix H: Different ANSYS Modelling Suite

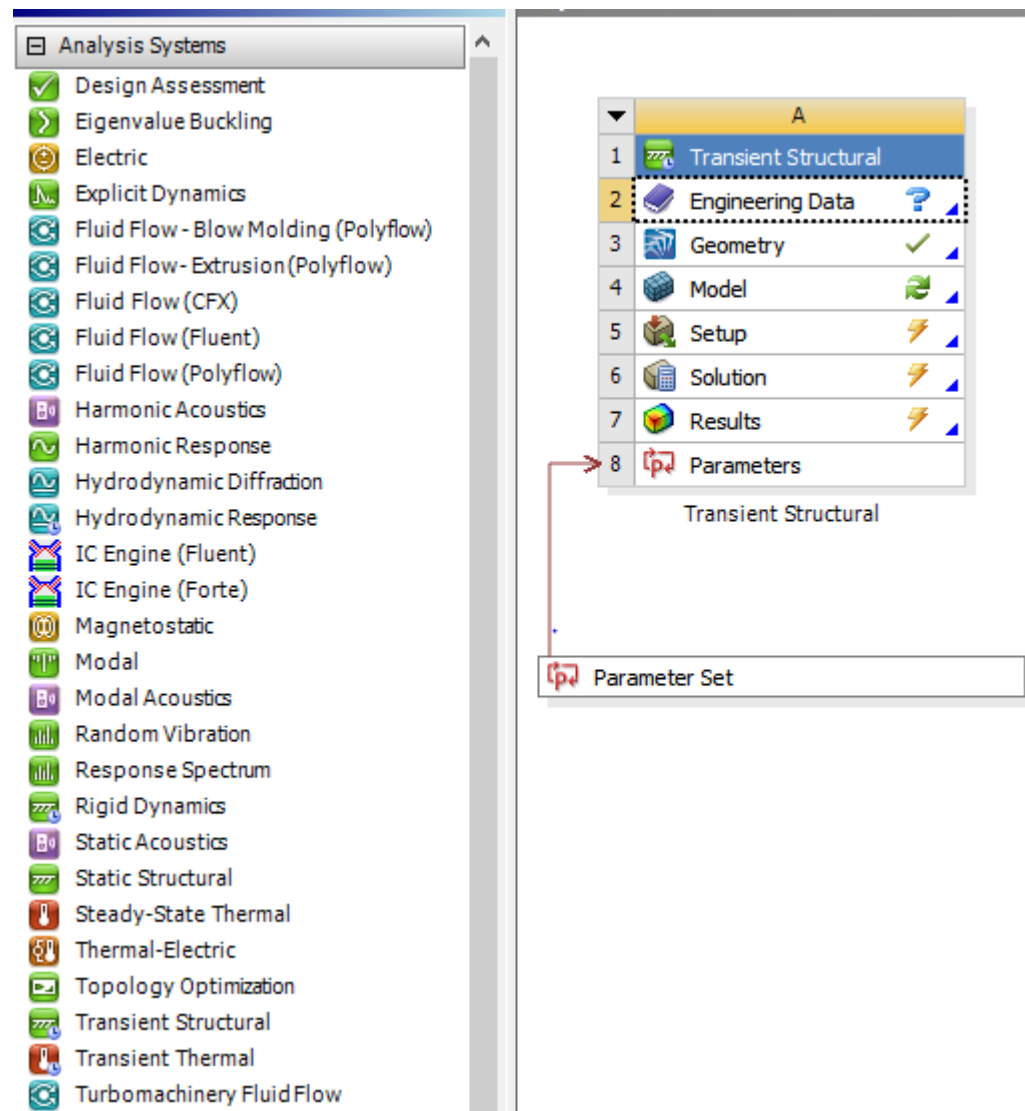


Figure 42 ANSYS Product suite